Organic Nanowire Fabrication and Device Applications

*Sung-Yong Min, Tae-Sik Kim, Yeongjun Lee, Himchan Cho, Wentao Xu, and Tae-Woo Lee**

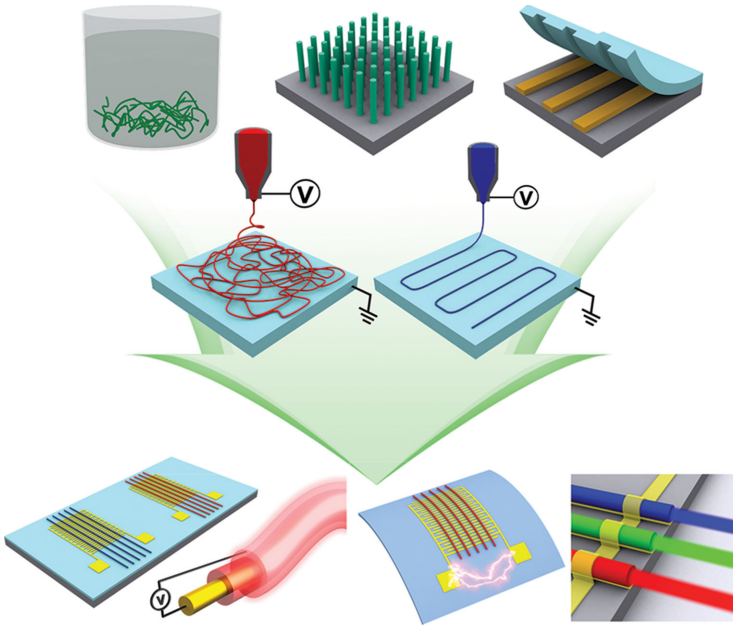

From the Contents

1. Introduction 46
2. ONW Fabrication Methods 46
3. Device Applications of Organic Nanowires 52
4. Conclusion 60

Organic nanowires (ONWs) are flexible, stretchable, and have good electrical properties, and therefore have great potential for use in next-generation textile and wearable electronics. Analysis of trends in ONWs supports their great potential for various stretchable and flexible electronic applications such as flexible displays and flexible photovoltaics. Numerous methods can be used to prepare ONWs, but the practical industrial application of ONWs has not been achieved because of the lack of reliable techniques for controlling and patterning of individual nanowires. Therefore, an "individually controllable" technique to fabricate ONWs is essential for practical device applications. In this paper, three types of fabrication methods of ONWs are reviewed: non-alignment methods, massive-alignment methods, and individual-alignment methods. Recent research on electronic and photonic device applications of ONWs is then reviewed. Finally, suggestions for future research are put forward.

1. Introduction

Electronic devices based on nanomaterials have focused on one-dimensional (1D) structures due to their excellent physical and electrical properties.[1–3] In particular, device applications of 1D organic nanostructures from π-conjugated small molecules or polymers have several advantages such as easy fabrication, low cost, high throughput, compatibility with flexible substrate, and tunability of electrical properties in molecular structure.[4–6]

Organic nanowires (ONWs) facilitate superior device performance due to enhanced π–π conjugated morphology[7,8] and the establishment of charge transport according to the molecular packing orientation[9,10]; consequently, they are favorable for applications in future electronic devices. Also, highly-integrated and highly-efficient energy-harvesting devices can be fabricated due to the extremely high aspect ratio and large surface-to-volume ratio of ONWs.[11,12]

Practical device applications of ONWs require several factors: i) alignment; ii) individually-controlled patterning; iii) reproducibility; and iv) controllability of wire morphology and chain orientation. Numerous methods have been used to prepare ONWs, including physical vapor transport,[4,13] solution-phase self-assembly,[5] template-assisted method,[14,15] soft-lithography[16] and electrospinning.[17] (**Figure 1**). However, practical industrial applications of ONWs are still limited because of the lack of a reliable technique which satisfies all of these requirements. Especially, the alignment of ONWs is very important for the aspect of industrial applications. Because the reliable technique which can control the precise number of nanowires (NWs) at desired position is essential for high-integration over large area and uniformity of each device. Hence, the alignment methods for inorganic NWs have been widely developed such as contact printing technique.[2]

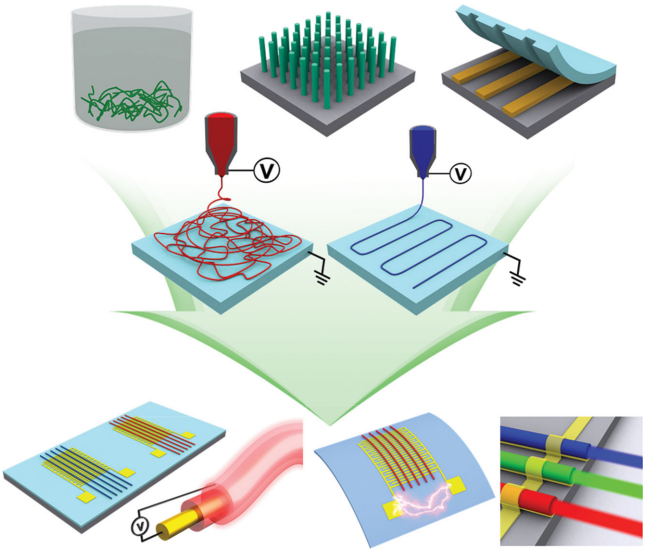

Figure 1. Numerous methods to prepare ONWs and (opto-) electronic device applications of ONWs (fabrication of wire transistors, light-emitting devices, energy harvesting devices, waveguide or lasing devices via solution-phase self-assembly, template-assisted method, soft lithography, electrospinning and electrohydrohynamic nanowire printing).

In this review, we introduce several fabrication methods of ONWs classified into three types according to capability of alignment: i) non-alignment methods; ii) massive-alignment methods; and iii) individual-alignment methods. Non-alignment methods need an additional aligning or positioning technique because the ONWs are not aligned during the wire fabrication process. Massive-alignment methods are techniques that can fabricate a massively-aligned ONW pattern; however, defining and characterizing individual wires are difficult tasks when these methods are used. Individual-alignment methods are processes that can individually control single ONW, and do not require additional patterning processes. Then we review recent progress in research into electronic and photonic device applications of ONWs. Finally, we summarize the review and outline possible future research perspectives. 1D organic nanostructures are variously classified according to their morphology, such as nanowires, nanoribbons, nanorods, nanofibers, nanotubes, and nanobelts; for convenience, we regard them all as ONWs.

2. ONW Fabrication Methods

2.1. Non-alignment Methods

2.1.1. Physical Vapor Transport

Physical vapor transport (PVT) has been widely used for fabricating organic single crystals with excellent electrical and optical properties.[18–21] However, PVT have drawbacks, including low throughput of device fabrication, high-temperature processes, and narrow material selectivity.[4]

ONWs fabricated using PVT have mainly consisted of copper phthalocyanine (CuPc) and copper hexadecafluorophthalocyanin (F_{16}CuPc) due to their thermal and chemical stability (**Figure 2**).[13,22–26] During the PVT process, growth occurs along a face with strong attractive interactions, i.e., the π–π stacking direction between organic molecules,[25] and the resulting NWs have a high aspect ratio.

Single-crystal ONWs grown by PVT are promising candidates for high-performance electronic applications because the crystals have limited disorder and no grain boundaries. However, for device applications, additional positioning processes are required such as stamping[19,27] or micro-manipulating[13,22,24] techniques, because controlling

S.-Y. Min, T.-S. Kim, Y. Lee, H. Cho,
Dr. W. Xu, Prof. T.-W. Lee
Department of Materials
Science and Engineering
Pohang University of Science
and Technology (POSTECH)
Pohang 790–784, Republic of Korea
E-mail: twlee@postech.ac.kr

DOI: 10.1002/smll.201401487

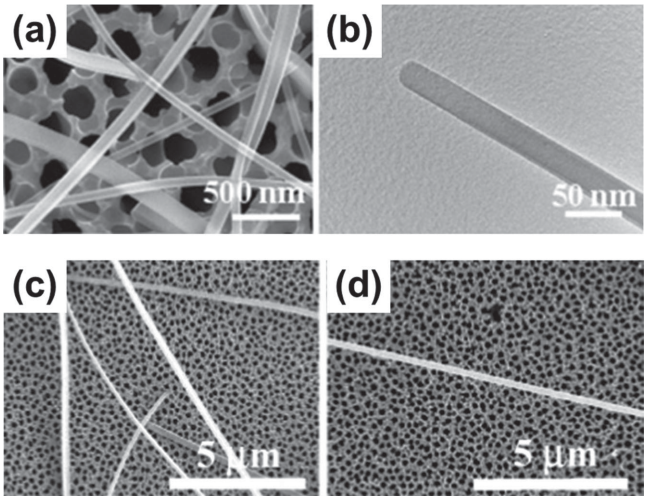

Figure 2. (a) Scanning electron microscope (SEM) and (b) transmission electron microscope (TEM) image of CuPc nanoribbons synthesized by the PVT technique. Reproduced with permission.[22] 2006, Wiley-VCH. (c,d) SEM images of F_{16}CuPc nanoribbons. Reproduced with permission.[23] 2006, American Chemical Society.

the precise direction and position of wire growth during PVT is a difficult task. For instance, Tang et al.[22] used PVT to prepare CuPc nanoribbons for transistor fabrication, and used a microprobe to transfer the nanoribbons to the device substrate (Figure 2a,b). In addition, Tang et al.[23] fabricated F_{16}CuPc nanoribbons directly on Si/SiO_2 substrate without any transfer process, but because the nanoribbons were randomly grown on the substrate, an alignment process using a microprobe was required, to deposit the electrodes exactly on top of the ribbons (Figure 2c,d). These additional positioning processes have low throughput, which limits their value in industrial electronic device applications.

2.1.2. Solution-Phase Self-Assembly

Solution-phase self-assembly has been used to fabricate 1D organic nanostructures which have the strong π–π stacking between organic molecules.[5] This self-assembly exploits the low solubility of an organic material in a poor solvent to induce precipitation or recrystallization. ONWs prepared in this way are obtained by cooling the solvent,[28] by adding a non-solvent,[7,8,29,30] or by cooling of a marginal solvent[31] (**Figure 3**).

Briseno et al.[28] fabricated hexathiapentacene (HTP) NWs by cooling a hot HTP solution in benzonitrile solvent. HTP is insoluble in most organic solvents at room temperature, but can be dissolved at higher temperatures and precipitated as bulk quantities of NWs by cooling the solution. The synthesized HTP NWs are collected and dispersed into poor solvent (Figure 3a,b). From transmission electron microscope (TEM) diffraction pattern, *d*-spacing of (100) and (010) plane were determined as 3.84 and 14.5 Å, respectively, which were corresponding with single-crystal grown from vapor-process. By dropping the dispersion of ONWs on the device substrate, ONWs can be obtained for device applications. However, the NWs deposited by dropping require an additional alignment process, because they are randomly scattered (Figure 3c).

Sung-Yong Min received his B.S. in Materials Science and Engineering in 2010 from Pohang University of Science and Technology (POSTECH). He has been a graduate student in POSTECH since 2010. His current research work is focused on controllable organic nanowires for nanolithography and large-area electronic applications.

Tae-Sik Kim received her B.S. in Materials Science and Engineering in 2008 from Chungnam National University. She has been a graduate student in POSTECH since 2008. Her current research work is focused on controllable organic and inorganic nanowires for nano-electronic applications.

Tae-Woo Lee is an associate professor in the department of the Materials Science and Engineering at POSTECH, Korea. He received his PhD in Chemical Engineering from Korea Advanced Institute of Science and Technology (KAIST), Korea in February 2002. He then joined Bell Laboratories, USA, as a postdoctoral researcher in 2002. From September 2003 to August 2008, he worked in Samsung Advanced Institute of Technology as a member of research staff. He received a prestigious Korea Young Scientist Award from the President of Korea in 2008 and The Scientist of the Month Award from the Ministry of Science, ICT and Future Planning in 2013. His research focuses on printed and organic electronics based on organic and carbon materials for flexible electronics, displays, solid-state lightings, and solar energy conversion devices.

Qiu et al.[31] induced selective phase separation and self-assembly of poly(3-hexylthiophene) (P3HT) by dissolving a P3HT/polystyrene (PS) blend in a marginal solvent such as dichloromethane at 40 °C and spin-casting at room temperature (Figure 3d). A nanofibrillar network of P3HT was formed in the PS matrix due to the low solubility of P3HT in a marginal solvent at room temperature (Figure 3e,f). This method has the advantage that it can prepare highly-crystalline NWs from a very small amount of P3HT, and that the NWs have high environmental stability due to the use of an embedding matrix as an encapsulation layer.

Another strategy for solution-phase self-assembly is to add organic solution to a poor solvent.[7,8,29,30] Balakrishnan et al.[29] prepared self-assembled perylene tetracarboxylic diimide (PTCDI) NWs by minimal injection of a concentrated chloroform solution of PTCDI into methanol. Also,

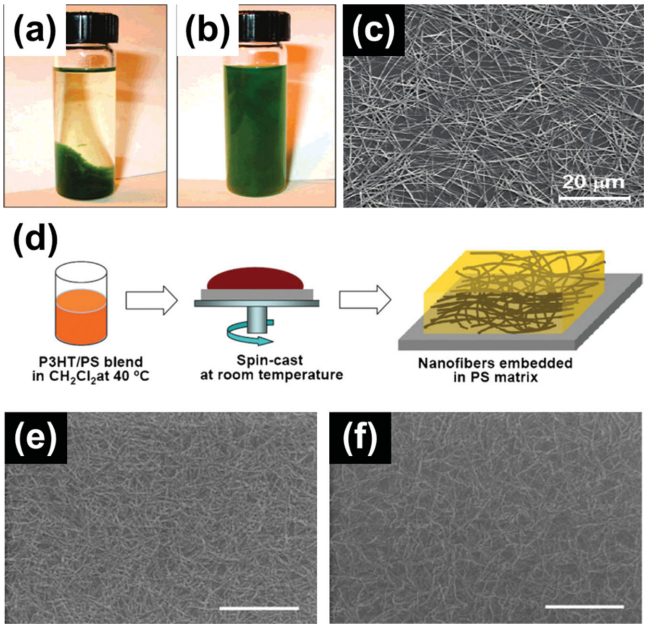

Figure 3. (a) Optical photograph of HTP NWs, and (b) well-dispersed NWs after agitating the vial. (c) SEM image of a network of HTP NWs. Reproduced with permission.[28] 2007, American Chemical Society. (d) Schematic representation of the formation of a P3HT nanofibrillar network in the PS matrix. (e,f) Films spin-cast from CH_2Cl_2 with different P3HT contents: (e) 10 wt% and (f) 5 wt%, scale bar is 1 mm. Reproduced with permission.[31] 2009, Wiley-VCH.

by using a mixture of good solvent and poor solvent, ONWs can be formed by π–π stacking in a poor solvent,[32] because aggregation or solidification of organic materials is induced when the concentration of the poor solvent is high. Besides cooling and addition of poor solvent, various approaches such as solvent exchange by vapor diffusion[33] and gelation of molecules with multiple long alkyl side chains[34] have been studied for preparing self-assembled ONWs.

Using solution-phase self-assembly, highly-crystalline ONWs can be easily prepared with high throughout compared with any other methods. However, device fabrication with self-assembled ONWs has the problem of low reproducibility due to sample-to-sample variation, because the wires are randomly dispersed in the solvent. Oh et al.[8] suggested a novel process for alignment of self-assembled organic wires, called filtration-and-transfer (FAT). PTCDI microwires (MWs) were aligned by fluid flow through a polydimethylsiloxane (PDMS) mask in vacuum filtration setup with a porous anodized aluminum oxide (AAO) membrane (**Figure 4**a). By using this method, the location and density of aligned organic wires can be controlled on a massive scale (Figure 4b,c). This approach is significant because it suggests the possibility of using ONWs for various device applications.

2.2. Massive-Alignment Methods

2.2.1. Template-Assisted Method

Template-assisted methods use a porous membrane as a template to fabricate the 1D nanostructures. Track-etched polycarbonate or AAO are mainly used as the porous

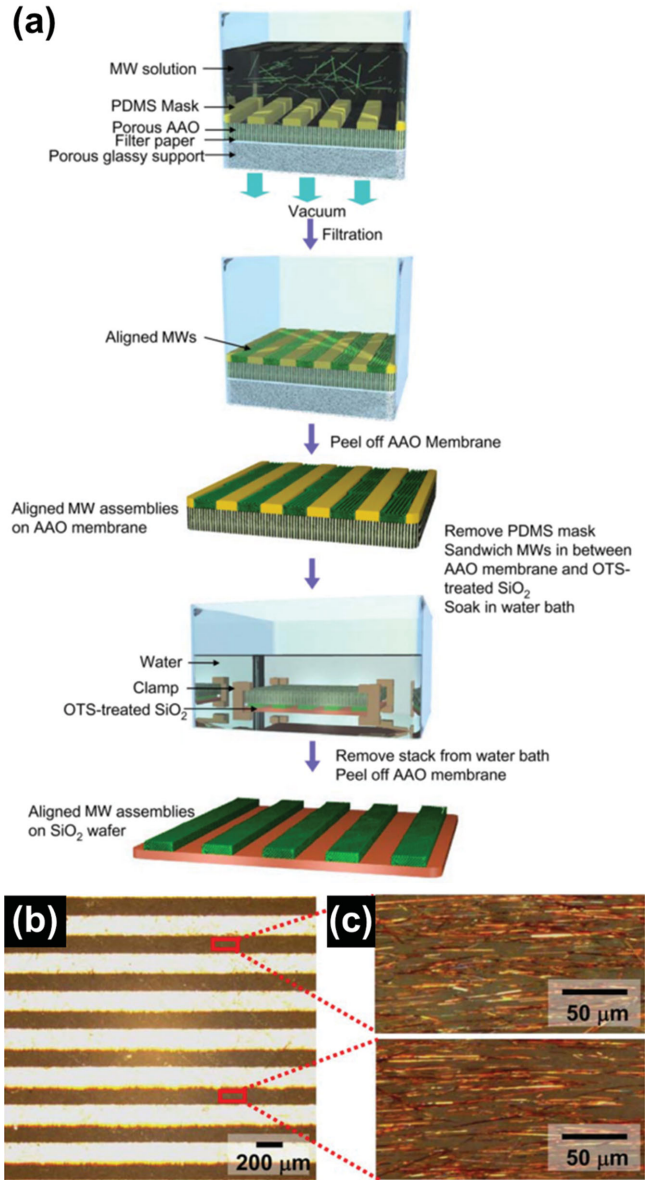

Figure 4. (a) Schematic diagram for FAT alignment of organic wires. (b) Bright-field optical image of aligned PTCDI MWs on an AAO membrane. (c) Zoom-in optical images of MWs in 2 different regions. Reproduced with permission.[8] 2009, National Academy of Sciences.

template. Especially, use of an AAO membrane has been studied due to its uniform pore arrangement.[35] Template-assisted methods have some advantages: simple preparation of porous membranes, easy control of wire diameter by adjusting pore size, wide selectivity of materials, and highly-ordered orientation. The only requirement of template-assisted method for ONWs fabrication is the loading of materials into the pore of template. It makes this method easily applicable to various applications based on ONWs. Various research has evaluated the possibility of using porous membranes as templates, such as Ni, TiO_2, MnO_2, V_2O_5, Co_3O_4, ZnO, CoPt, Lead Zirconate Titanates, $BaTiO_3$, and SiO_2[36–42] when preparing ONWs. Fabrication of ONWs by the template-assisted method is classified into two types: electrophoretic deposition[38–41,43] and template wetting.[14,15,44–46]

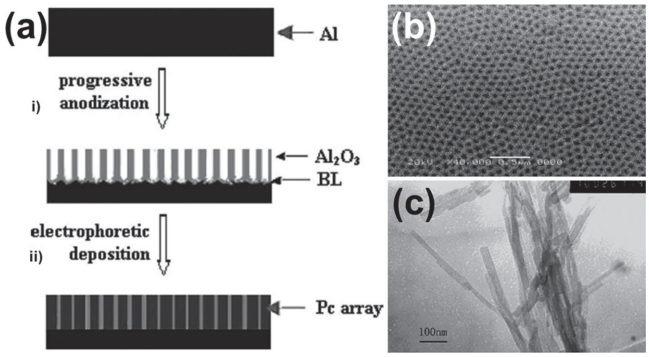

Figure 5. (a) Diagram for the preparation of anodic AAO template and CuPc NW array via electrophoretic deposition (BL: barrier layer, Pc: phthalocyanine). (b) SEM image of the cross section of a blank AAO template. (c) TEM image of the CuPc NWs through AAO template. Reproduced with permission.[43] 2005, Elsevier B.V.

Electrophoretic deposition exploits the oriented motion of charged particles by coating materials from an organic solution onto a porous membrane.[35,39] Xu et al.[43] reported the first deposition of a CuPc NW array by electrophoretic deposition using a porous AAO template (**Figure 5**). Density and morphology of NWs are strongly dependent on concentration of solution, zeta potential, applied electric field, reaction kinetics, and therefore can be easily controlled by adjusting various experimental parameters. Electrophoretic deposition can be also used to synthesize polymers from monomers.[47] By controlling the reaction kinetics, various structures from nanotubes[48] to NWs[47] can be formed.

The template wetting method uses a porous membrane that has been wetted with a melted polymer or a solution.[14,15,44–46] When the porous membrane is placed on the polymer melt or solution, a thin film covers the pore wall due to high surface energy of the membrane.[15,44] This simple approach was first proposed by Steinhart et al.[15] Because the adhesive force for wetting is stronger than the driving force for complete filling, nanotubes are formed dominantly. However, by controlling the pore size and wettability, completely-filled NWs can be also formed.[49] O'Carroll et al.[44] fabricated poly(9,9-dioctylfluorene) NWs using the melt-assisted template wetting method, and demonstrated that they can lase if photo-pumped.

ONWs formed by template-assisted methods have the same arrangement as the pore distribution. By selective etching of templates, a highly-uniform vertically-aligned ONW array can be obtained. Although some paper have reported device applications that use a vertically-aligned NW array as synthesized,[45,50] for practical device applications an additional horizontal alignment process is required, such as contact printing with unidirectional massive-alignment.[51]

2.2.2. Soft Lithography

To fabricate ONWs, top-down approaches based on lithography have also been reported for use in fabricating devices based on organic semiconductors. Soft lithography techniques cause less damage to organic materials than do conventional photo- or electron-beam lithography. Soft lithography is not a specific process, but a collective term that describes techniques based on molding or stamping without using light, electron- or ion- beam.[52]

Soft lithography for nanofabrication includes a great variety of techniques such as contact printing,[53] replica molding,[52,54] imprint lithography (embossing),[55–63] and transfer molding; new methods of soft lithography are proposed often. Compared with conventional lithography, soft lithography has several advantages: i) elimination of some factors that limit the resolution in conventional lithography such as optical diffraction and optical transparency; ii) low processing cost; and iii) high throughput.[16,64] However, use of soft lithography for nanofabrication faces some constraints: i) the practicality of fabricating a master mold that has a nano-pattern; ii) distortion near the edge of the pattern; iii) limited lifetime of the mold; iv) difficulty of aligning the pattern during multilayer fabrication; and v) residue after patterning.[64–67]

As an ONW fabrication method that does not leave a residue layer, Duan et al.[68] reported the nanomolding in capillary (NAMIC) method that is similar to the micromolding in capillary method.[69] NAMIC uses a stamp fabricated by nanoimprint lithography (NIL) with a thermal resist on a flat PDMS substrate that has nanogrooves of 50- or 100-nm width (**Figure 6**a). The advantages of NAMIC are that well-defined sub-100-nm patterns can be formed over a large area in a short time, and that various materials can be used to prepare the nano-patterns. Fluorescent dye molecules (tetramethylrhodamine isothiocyanate), protein molecules, SiO_2 nanoparticles and polymers have been used to form continuous nanolines or wires with sub-100 nm width and height. Conductive poly(3,4-ethylenedioxythiophene) doped with poly(styrene sulfonate) (PEDOT:PSS) NWs with a width of 100 nm and a height of 90 nm were prepared using NAMIC and showed resistance similar to a bulk PEDOT:PSS layer (Figure 6b). This result shows the great potential of NAMIC for electronic applications.

Liquid-bridge-mediated nanotranfer molding (LB-nTM)[70] is another nano-patterning method that does not leave a residue layer. LB-nTM is similar to conventional microtransfer molding,[65] but a mold with solidified ink is pressed directly on the surface of a substrate covered by a polar liquid layer, not on a bare surface (**Figure 7**). The polar liquid layer forms a liquid bridge and works as an adhesion layer between the solidified ink and substrate. Unlike other methods to pattern nanostructures directly, LB-nTM can fabricate nano-patterns without leaving any residue and can adjust the position of the mold even after it contacts the substrate, because the solidified inks are not transferred onto the substrate before drying of polar liquid. Using LB-nTM, zinc-tin oxide NWs and 6,13-bis(triisopropylsilylethynyl) pentacene (TIPS-PEN) NWs with sub-100-nm width were successfully formed.[70]

2.2.3. Electrospinning

Electrospinning (ES) is a well-known ONW fabrication method that uses an electric field. ES employs electrostatic force to stretch a viscous polymer solution into NWs

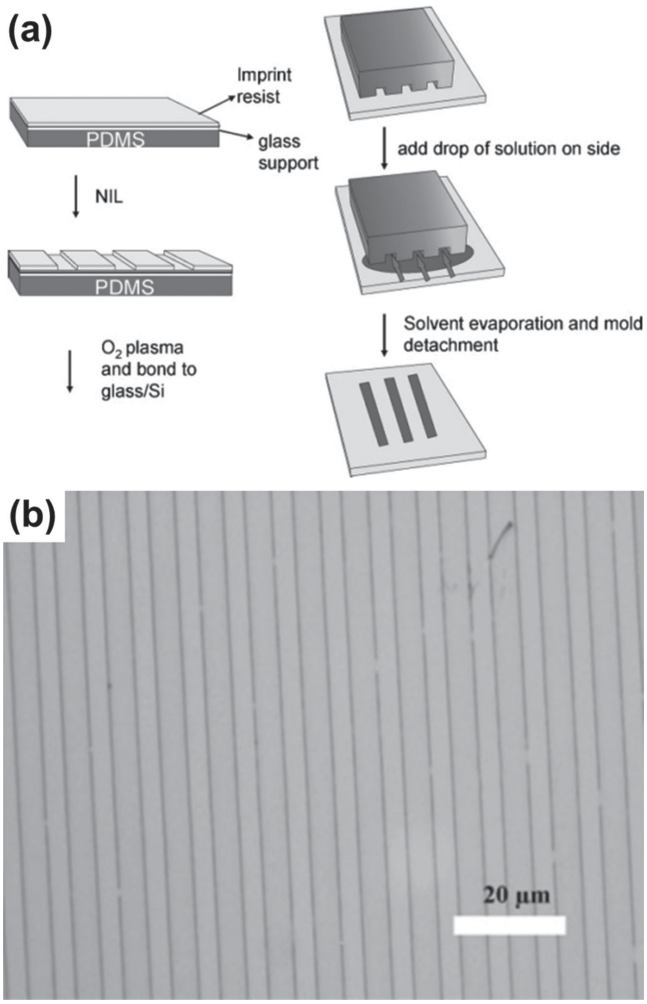

Figure 6. (a) Process scheme for NAMIC. (b) Optical microscopy of PEDOT:PSS NWs by NAMIC. Reproduced with permission.[68] 2010, Wiley-VCH.

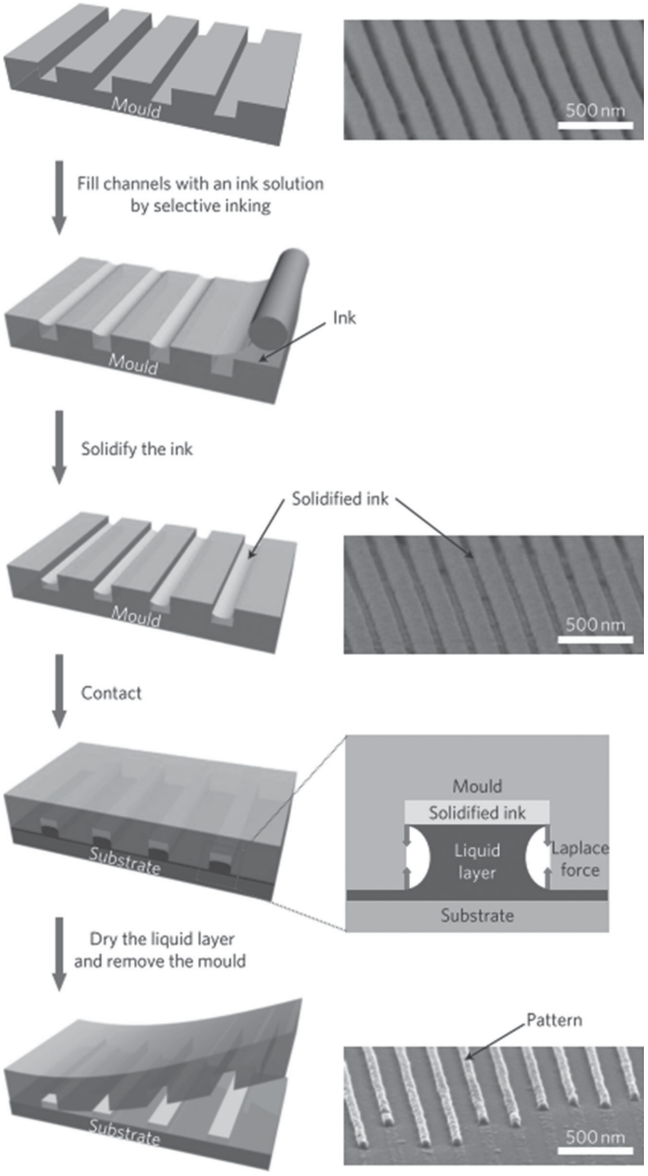

Figure 7. Schematic illustration of LB-nTM. Reproduced with permission.[70] 2010, Nature Publishing Group.

(**Figure 8**a). ES can fabricate ONWs easily with simple equipment, and can precisely control the morphology and diameter of wires. The diameter of the wire is determined by various experimental parameters such as solution concentration, flow rate, voltage and nozzle-to-collector distance.[17a] To control NW diameter, solution concentration is particularly important because it determines the viscosity of the polymer solution.

During stretching of the polymer solution in ES, electrospun NW shows a chaotic whipping motion (bending instability) due to the electrostatic interaction between the external field and the charges in the jetted solution.[71–73] Because of the chaotic whipping and high wire formation speed, electrospun wire is collected as a randomly coiled mat (Figure 8b). Hence, electrospun NWs have been generally used as a non-woven mat in various applications such as filtration,[74–78] bio-engineering[79,80] and sensors.[81–83] ES has attracted attention in electronic device applications based on electrospun organic semiconducting NWs, but its usefulness is limited by the randomly coiled nature of the NWs produced. Therefore, methods to align the NWs have been studied for various applications.[71,74]

Several groups introduced methods to align wires on a rotating drum-type collector.[84–87] This method prevents twisting of the wire by winding it around a rapidly-rotating drum or cylinder. This method can align NWs using fairly simple equipment, but it has the drawbacks that matching the speed of wire formation and collector rotation, and controlling the position of aligned NWs are difficult tasks.

Several research groups have demonstrated a novel method that uses multiple collectors to align the electrospun NWs.[88–91] This method can generate uniaxially-aligned NWs between more than two flat- or blade-type collectors arranged with regular spacing (Figure 8c,d). During deposition, NWs are pulled and aligned by the electrostatic attraction of each collector. According to this principle, Li et al.[89] fabricated various NW array patterns using multiple collectors with different orientations. Also, Jalili et al.[92] investigated how the degree of alignment depends on the applied

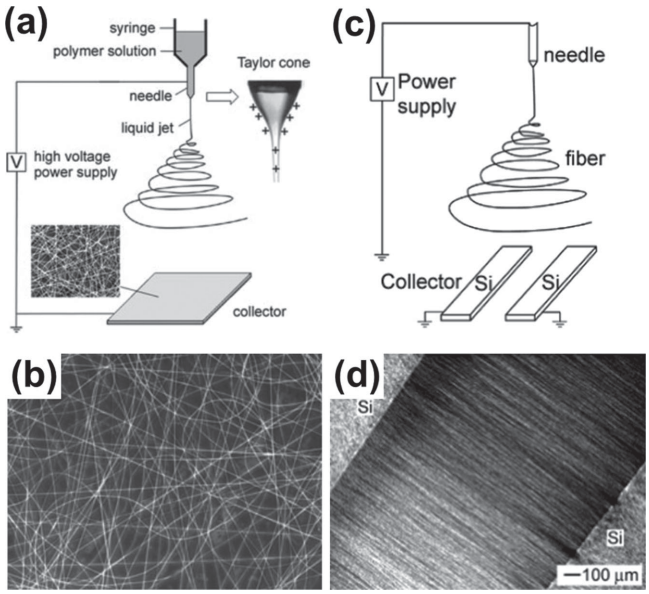

Figure 8. (a) Schematic illustration of the basic setup for ES. (b) SEM image of electrospun poly(vinyl pyrrolidone) NWs. Reproduced with permission.[71] 2004, Wiley-VCH. (c) Schematic illustration of the setup for ES to generate the uniaxially aligned NWs using two silicon strips as collectors. (d) Optical micrograph of aligned nanofibers two silicon stripes. Reproduced with permission.[88] 2003, American Chemical Society.

voltage and the width of the gap between multiple collectors. The multiple-collector method[93,94] has been widely used to fabricate NW-based devices due to its simplicity and higher degree of orientation than that of the drum-type collector method. New strategies for alignment of electrospun NWs are continually being developed; these methods include suppression of bending instability by using a biased ring,[95,96] by switching of biased multiple collectors,[97] or by alignment of wires with a magnetic field.[98]

2.3. Individual Alignment Methods

2.3.1. Meniscus-Guided Printing

Meniscus-guided printing (MGP) is a method that prints the desired materials while maintaining the solution meniscus formed between glass pipette and substrate. Unlike conventional probe-based drawing,[99,100] MGP can easily supply the ink solution by using a micro- or nano-sized glass pipette,[101] and can print the nanostructures over a large area. MGP can also fabricate thinner wire compared with direct ink writing[102–104] because MGP does not use colloidal ink particles.

The best feature of MGP is that three-dimensional (3D) wire patterning is possible. Because the meniscus between the pipette tip and the growth front of deposited wire is maintained after the deposited solution solidifies, a 3D nanopattern can be formed. Suryavanshi and Yu[101,105] and Hu and Yu[106] used MGP and electrochemical deposition to fabricate freestanding metal NWs. Using electrolyte solution mixed with metal ions as an ink and applying an electric field between pipette and substrate, Cu and Pt NWs with freestanding or bridge structure were printed. The size and shape of the meniscus are defined by the size of the nozzle, the thermodynamic properties of the solution, the distance between the pipette tip and the growth front, and the pulling speed. The size of the meniscus determines the diameter of the deposited wire. Hu and Yu[106] used a glass pipette with a nozzle diameter of ~100 nm to fabricate Pt NWs with a diameter of 120 nm and length of 6.8 μm.

Kim et al.[107] used MGP to demonstrate the first 3D patterned-conducting polymer NW. They formed polypyrrole (PPy) NWs by oxidative polymerization of pyrrole monomer solution as an ink (**Figure 9**a). The diameter of the wire was controlled to a minimum of 50 nm by the pulling speed of pipette and by the flow rate of monomer solution. Different lengths and shapes (e.g., straight, complex-shape, branches and bridges) of 3D PPy nanostructures were demonstrated by moving the meniscus (Figure 9b,c). Kim et al.[108] also reported a 3D patterned nanoarch of PEDOT:PSS NWs for stretchable electrical interconnection and transistor device with extreme stretchability up to 270%. These results show the great potential of 3D structured NWs for use in stretchable electronics.

MGP is a distinctive technique which can fabricate the 3D patterned ONWs in specific position. However, the wires are formed with very slow pipette pulling speed of less than 1 mm/s so that their device applications on large-area are limited due to the low throughput of wires. Therefore, a method which can prepare the ONWs with fast and simple process is required.

2.3.2. Electrohydrodynamic Nanowire Printing

Electrohydrodynamic nanowire printing (ENP)[109] is a novel technique to fabricate well-aligned and well-patterned

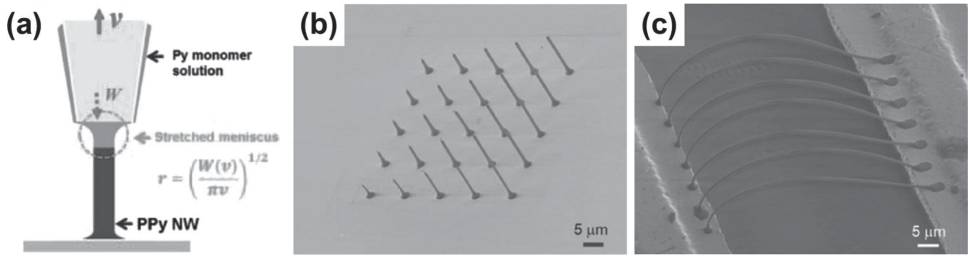

Figure 9. (a) Schematic explanation of PPy NW fabrication by MGP. The NW radius, r is controlled by the pulling speed, v; W(v) is the solution flow rate. (b) SEM images of an array of r ~350 nm PPy NWs array with lengths from 5 to 15 μm individually controlled by tuning the pulling time. (c) Array of nanoarch-bridges (r ~240 nm) between two Cu substrates separated by a ~50 μm gap. Reproduced with permission.[107] 2011, Wiley-VCH.

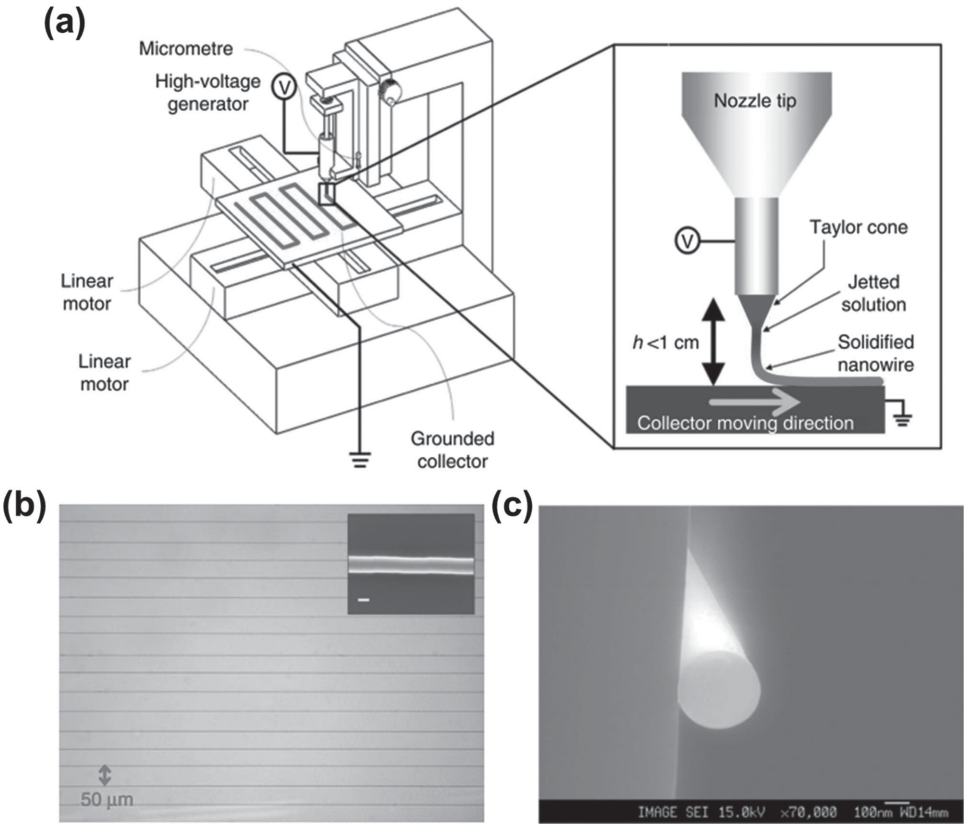

Figure 10. (a) Schematic diagram of ONW printer and NW printing process. (b) Optical micrograph of well-aligned PVK NWs. The diameter of PVK NW is 290nm (inset, scale bar, 200 nm). (c) SEM image showing cross section of well-aligned PVK NW, which forms a perfect circle. Reproduced with permission.[109] 2013, Nature Publishing Group.

ONWs. To fabricate the ONWs, ENP uses a principle similar to that of ES which applies an electric field to stretch the polymer solution. ENP can fabricate and align NWs by suppressing the bending instability. In conventional ES, the ejected polymer jet fluctuates randomly a few millimeters distant from the nozzle tip, and shows bending instability, which increases as the distance between nozzle tip and collector increases.[72] When the nozzle tip approaches the collector closely, NWs in straight-jet region can be obtained.[110,111] In ENP, if the nozzle is <1 cm from the collector and high voltage is applied, ONWs are deposited directly on the collector and aligned with the desired orientation by a high-speed linear stage (**Figure 10**a). ENP produced printed poly(N-vinylcarbazole) (PVK) NWs that had totally-parallel orientation with a regular spacing of 50 μm and a diameter of 290 nm (Figure 10b). The printed PVK NW had a perfectly circular cross section, which implies that the polymer jet was fully solidified during the deposition of wire (Figure 10c). By using ENP, the position and orientation of NWs can be individually controlled, and thereby overcome the limitations of NW alignment that occur when using ES. ENP also has high throughput, and can fabricate a very long (several meters) strand of NW in just a few seconds.

Min et al.[109] also demonstrated highly-aligned semiconducting ONWs and electronics device applications. Using ENP, the number of aligned NWs can be easily controlled. This means that the device characteristics can be controlled by adjusting the number of wires with the ENP technique. Therefore, ENP is one of the most promising approaches for well-controlled ONW fabrication in large area and for development of electronic device applications based on the ONWs.

3. Device Applications of Organic Nanowires

3.1. Field-Effect Transistors and Complementary Logic Circuits

3.1.1. Field-Effect Transistors

In this section, we review reports that describe the use of ONWs in electronic device applications. Field-effect transistors (FETs) are basic components that usually function as switches or amplifiers in electronic circuits. Also, FETs are commonly designed to measure the electrical characteristics of semiconducting ONWs. Critical parameters to evaluate a FET include its field-effect mobility and its current on/off (I_{on}/I_{off}) ratio.

Single Crystalline Nanowires: ONWs have an advantage in charge transport because their strong π–π interaction along the wire axis leads to high-performance FETs. Especially, FETs based on single-crystal ONWs show intrinsic charge-transport properties and the highest performance because of the absence of grain boundaries and the exceptionally high chemical purity. Therefore, significant progress has been made in fabrication of single crystals and high-performance organic single-crystal FETs.

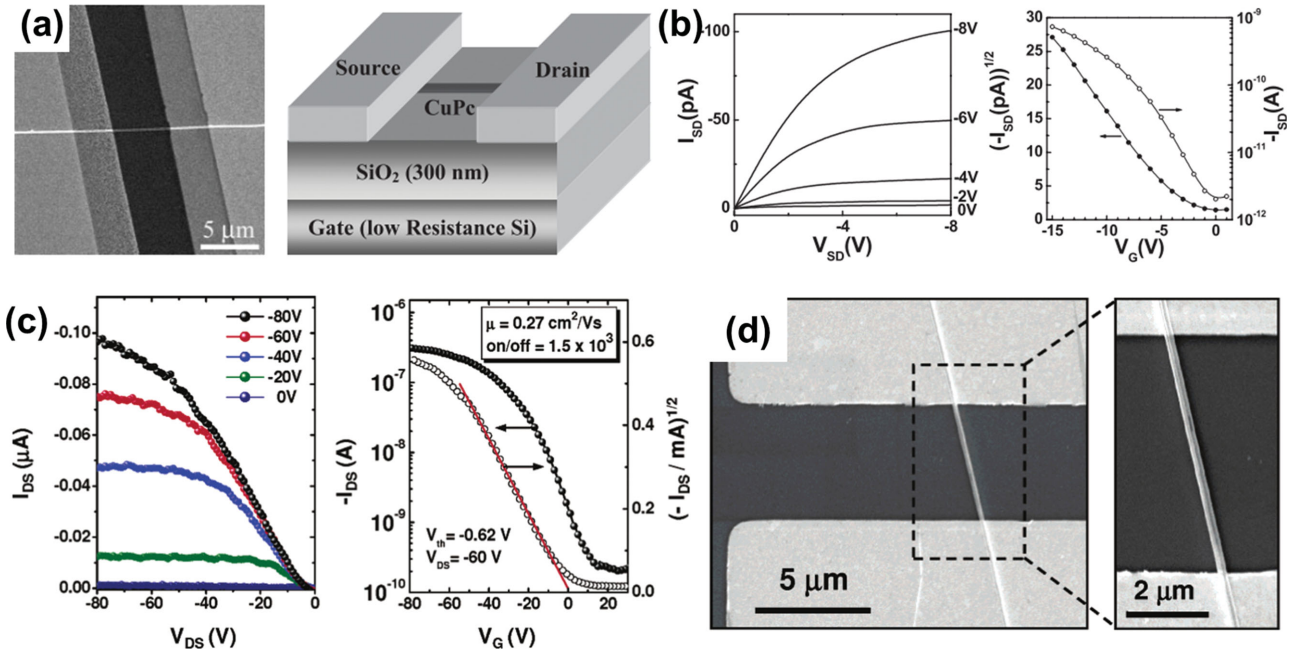

Figure 11. (a) SEM image and schematic diagram of an OFET based on an individual CuPc nanoribbon. (b) Output and transfer characteristics of the nanoribbon FET measured at a fixed source–drain voltage V_{SD} = 10 V. Reproduced with permission.[22] 2006, Wiley-VCH. (c) Output and transfer characteristics of a HTP single-NW transistor. (d) SEM image of a representative bottom-contact HTP NW FET. The inset shows a magnified view of the HTP NW bridging the source-drain gold electrodes. Reproduced with permission.[28] 2007, American Chemical Society.

Vapor growth process (i.e., PVT) is a general method to produce high-quality crystals.[13,22–24,112,113] Several research groups have recently demonstrated successful fabrication of organic FETs (OFETs) using single-crystal NW synthesized by PVT. Tang et al.[22] used PVT to synthesize single-crystalline nanoribbons of CuPc, and fabricated OFETs based on individual nanoribbons (**Figure 11**a,b), which was the first OFET with single-crystalline ONW. The OFETs have low threshold voltage (<3 V) and high hole mobility (~0.1–0.2 $cm^2 \cdot V^{-1} \cdot s^{-1}$). The CuPc ribbons exhibit excellent flexibility and reproducibility, which indicate the great potential of ONWs for flexible or bendable electronics applications in the future. However, CuPc nanoribbons prepared by PVT had poor contact between the ribbon and SiO_2 dielectric because the ribbons should be transferred on the SiO_2 substrate to fabricate the FET. Poor optimization of contact resulted in lower mobility than FETs based on large CuPc single crystal with the mobility of 1.0 $cm^2 \cdot V^{-1} \cdot s^{-1}$.[114]

In order to overcome the poor contact issue, Tang et al.[23] prepared single-crystalline F_{16}CuPc nanoribbons with in-situ growth process on device substrate (Si/SiO_2), and fabricated high-performance air-stable n-type FETs (Figure 2c,d). Because the in-situ growth process surmounted the disadvantages of the handpicking process for fabrication of organic single-crystal devices and because the asymmetrical drain/source (Au/Ag) electrode configuration improved electron injection and transport, the achieved electron mobility values (~0.2 $cm^2 \cdot V^{-1} \cdot s^{-1}$) were the highest of single-crystal F_{16}CuPc ribbon FETs to date.

On the other hand, solution-phase self-assembly including recrystallization,[28] solvent-exchange,[7,8] and drop-casting assembly[30] provides facile and low-cost approaches for preparing single-crystal ONWs and high-performance FETs compared with PVT.[7,8,28,115–117] Briseno et al.[28] fabricated the HTP single-crystal NW from self-assembly in solution and achieved NW transistors by drop-casting of NW suspension on device substrate (Figure 11c,d). The transistors based on single HTP NW showed the mobility of 0.27 $cm^2 \cdot V^{-1} \cdot s^{-1}$ and I_{on}/I_{off} of ~1.5 × 10^3,[118] which was six times higher than that of vapor-deposited HTP thin film transistors (0.04 $cm^2 \cdot V^{-1} \cdot s^{-1}$). The authors also demonstrated the HTP NW FETs array over large area. After drop-casting of NW suspension, the substrate was tilted at a 45° angle to promote the alignment of NWs. However, this method was not completely successful. Due to the disorders such as random crossing or overlap of the NWs networks, large-area FET array showed the mobility of 0.057 $cm^2 \cdot V^{-1} \cdot s^{-1}$ which was 5-fold lower than that of single NW FET. It is concluded that the optimization of NW alignment is essential for device applications.

Self-assembled single-crystal NW FETs using other kinds of small molecules including TIPS-PEN,[7] anthracene-,[115] thienoacene-,[116] and perylene-derivatives,[30,117] have been also reported with excellent electrical characteristics. However, the ONWs fabricated by conventional solution-phase self-assembly were difficult to align on desired position, which affects as an obstacle for fabrication of large-area device arrays or induces a large deviation of performance between each device. To solve this problem, Park et al.[119] developed the one step process to generate single crystal ONW arrays using a direct printing method (LB-nTM) combining self-assembly and soft lithography techniques (refer to Figure 7). Well-aligned single crystal ONWs were synthesized by self-assembly within the nano-scale channels of molds due

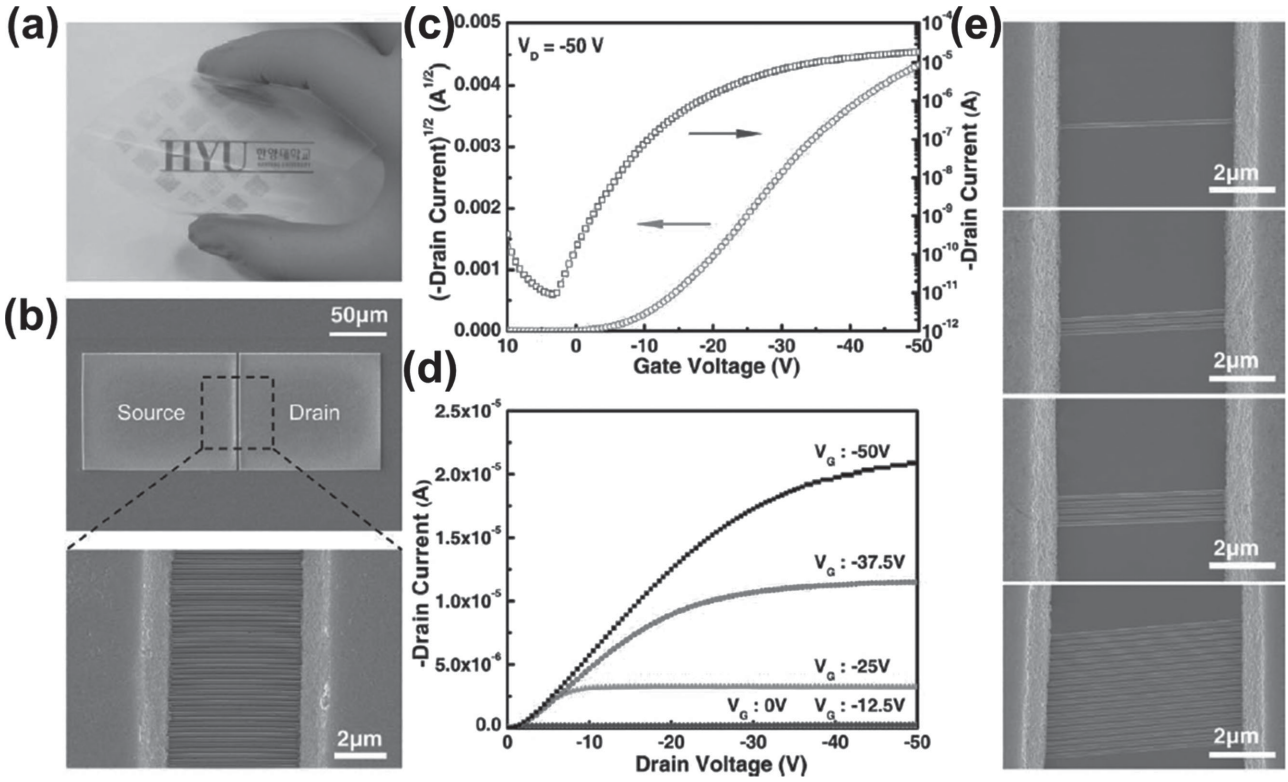

Figure 12. (a) Photograph of an array of single-crystal TIPS-PEN NW FETs on a flexible substrate. (b) SEM images of a TIPS-PEN NW FET showed the well-aligned TIPS-PEN NWs array channel between the electrodes. (c) Transfer curves and (d) output curves of the FETs with 90 TIPS-PEN NWs. (e) SEM images of FETs with 1 to 19 single-crystal TIPS-PEN NWs. Reproduced with permission.[119] 2013, Wiley-VCH.

to the nanoconfinement effect,[120] and these NWs could be transferred to desired position on the substrate by LB-nTM process. The authors demonstrated the single crystal ONW transistors using TIPS-PEN (**Figure 12**), C_{60}, and P3HT ink solutions and achieved field-effect mobilities of 1.52, 0.12, and 0.08 $cm^2 \cdot V^{-1} \cdot s^{-1}$, respectively.

Solution-processible and high performance n-type organic semiconductors are essential for the all organic and flexible complementary logic circuits. Oh et al.[8] used FAT to efficiently align organic wires and fabricated air-stable n-channel organic transistors with aligned single-crystal PTCDI MWs (Figure 4). The devices had I_{on}/I_{off} of ~2.9 × 10^5, and the highest measured mobility of 1.4 $cm^2 \cdot V^{-1} \cdot s^{-1}$. This result was the highest performance yet reported for n-channel transistors based on organic single crystal wires prepared by solution-phase self-assembly. It is comparable with the highest mobility of p-type ONWs prepared by self-assembly. The origin of these high values is the structural perfection of single-crystal MWs and the π-stacking direction which is parallel to the wire axis.

Semiconducting Polymer Nanowires: Until now, this review has just dealt with the OFETs of single-crystal semiconducting ONWs based on small molecules. The following also addresses the performance and techniques for ONW transistors with semiconducting polymer NWs. Semiconducting polymer NWs are also fabricated by various methods such as the solution-phase self-assembly, soft lithography and ES, etc. For example, Briseno et al.[121] used a solution-phase self-assembly process to fabricate poly(benzobisimidazobenzophenanthroline) (BBL) nanobelts-based FETs and observed electron mobility of up to 0.007 $cm^2 \cdot V^{-1} \cdot s^{-1}$ and I_{on}/I_{off} of ~1 × 10^4. However, self-assembled polymer NWs are randomly oriented because external forces that can align the NWs are absent.[31,32,122]

ES is a representative method of external force-driven self-assembly which can form individual NWs on a massive scale.[6,89] FETs based on the electrospun NWs have been intensively studied since Pinto et al.[123] introduced the first electrospun NW FET using a blend of doped polyaniline (PANi) and poly(ethylene oxide) (PEO). In the early stage of electrospun NW FETs, the wires were collected just by passing the sample substrate quickly between the nozzle and the grounded collector,[123,124] resulting in poor alignment of wires and low reproducibility of NW FETs. To align the electrospun conjugate polymer NW, rotating collector[125] or multiple collectors[93,94] have been used. For example, Lee et al.[93] collected electrospun pure P3HT nanofibers and blend P3HT nanofibers with poly(ε-caprolactone) (PCL) between two parallel metal wires (~3 cm apart) and transferred the fibers on the device substrate. FETs based on single nanofibers of pure P3HT and P3HT/PCL blend showed the hole mobilities of 0.017 $cm^2 \cdot V^{-1} \cdot s^{-1}$ and 0.0012 $cm^2 \cdot V^{-1} \cdot s^{-1}$, respectively. They also fabricated high performance ion-gel gated OFETs based on electrospun P3HT/PCL blend nanofibers which were aligned by parallel metal wires with the field-effect mobility of ~2 $cm^2 \cdot V^{-1} \cdot s^{-1}$ and the I_{on}/I_{off} of ~10^5 (**Figure 13**a,b).[94] By controlling the number of collected fibers, the electrical properties of FETs were successfully adjusted.

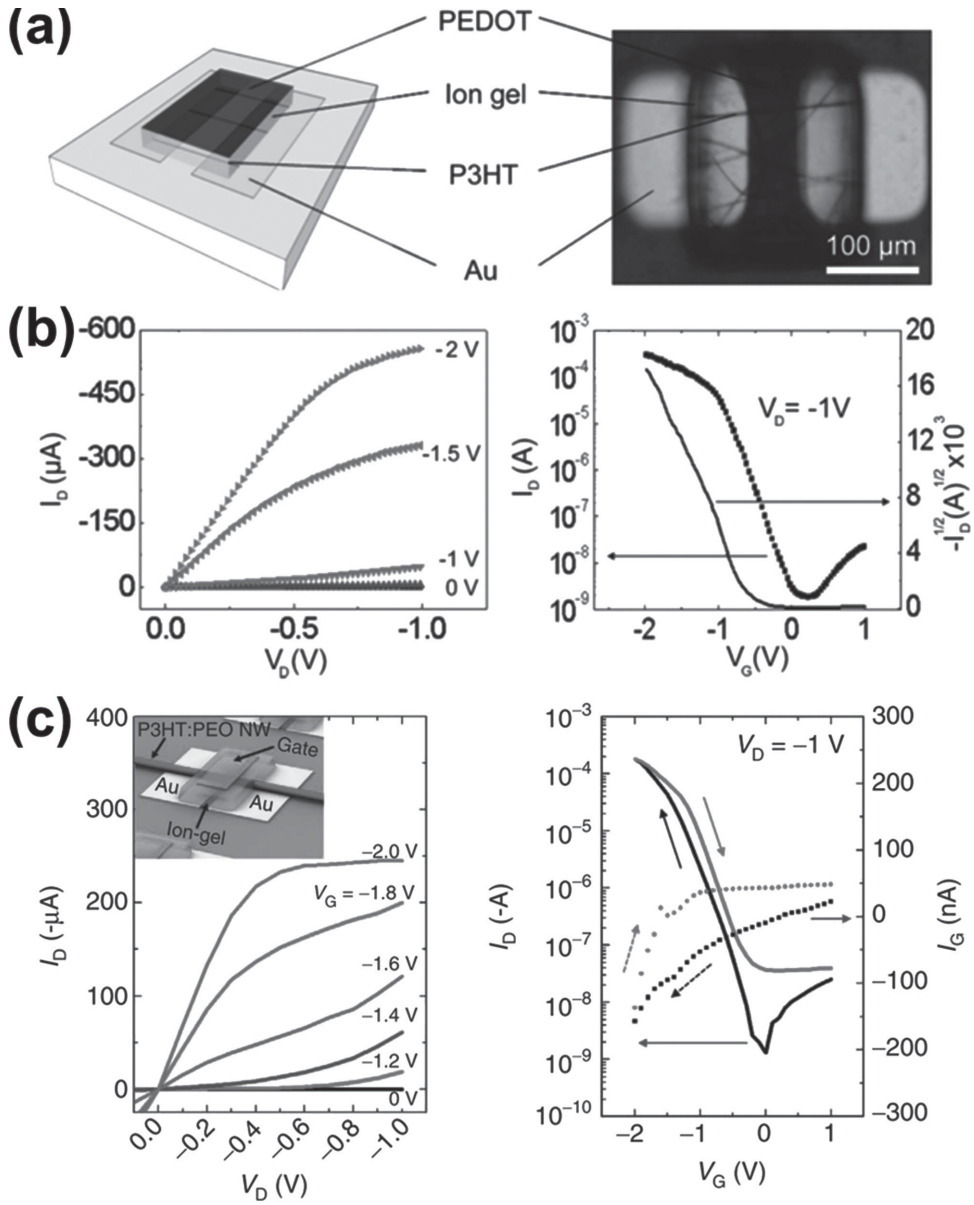

Figure 13. (a) The scheme and the optical microscopy image of an arrayed transistors based on P3HT NW. (b) Output and transfer characteristics of the arrayed OFET. Reproduced with permission.[94] 2010, American Chemical Society. (c) Output characteristics (left, inset: device structure), and transfer characteristic (right, solid line) and gate current versus gate voltage characteristics (right, dot line) of P3HT/PEO-blend (70/30, w/w) NW and nano-channel FET based on the ion-gel gate dielectric. Reproduced with permission.[109] 2013, Nature Publishing Group.

Chen et al.[126] also prepared the aligned P3HT nanofibers using coaxial ES technique and aluminum disk collector with rectangular hole, and explored crystalline structure and chain orientation of aligned nanofibers with wide-angle X-ray scattering, optical absorption and polarized photoluminescence. The author improved performance (hole mobility of 0.192 $cm^2 \cdot V^{-1} \cdot s^{-1}$ and I_{on}/I_{off} of 4.45×10^4) by analyzing the crystalline structure and orientation of P3HT chain in nanofibers with a suitable control of the shell flow rate and annealing temperature. This group extended their research by reporting the two-dimensional (2D) conjugated polythiophene derivative, poly{[2′,5″-5,5‴-di(2-ethylhexyl)-3′;5′,2″;4″,2‴]quaterthiophene-*alt*-3,6-dithien-2-yl-2,5-di(2-ethylhexyl)-pyrrolo[3,4-c]pyrrole-1,4-dione-5′,5″-diyl]} (P4TDPP).[127] The crystallinity, orientation, and molecular packing of P4TDPP nanofibers are significantly enhanced by a crystalline-induced procedure with the result that the average hole mobility of the P4TDPP electrospun nanofiber transistors was 0.305 $cm^2 \cdot V^{-1} \cdot s^{-1}$, and I_{on}/I_{off} was 1.30×10^5, higher than that of the spin-coated film device. Although Chen et al.[126] and Lin et al.[127] could align the nanofibers to characterize the properties in fibers, however, previously introduced alignment methods of electrospun NWs have still some problems: i) poor position and direction addressability of aligned NW; ii) low uniformity of device characteristics on large-area arrays.

Recently, Min et al.[109] solved the problem of precise control of polymer NWs (PVK, P3HT/PEO and poly{[*N,N′*-bis(2-octyldodecyl)-naphthalene-1,4,5,8-bis(dicarboximide)-2,6-diyl]-alt-5,5′-(2,2′-bithiophene)} (P(NDI2OD-T2) or

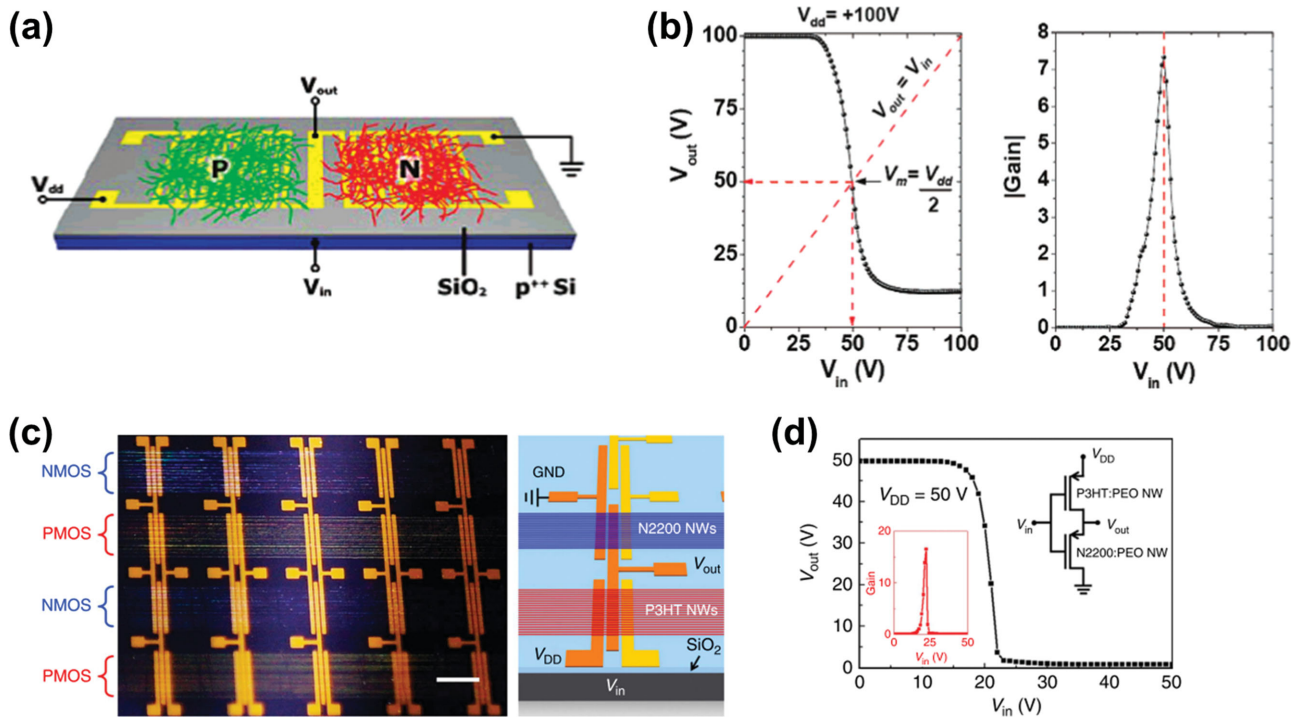

Figure 14. (a) Schematic of an inverter with p- and n-type NW networks covering interdigitated source-drain electrodes. (b) Static inverter transfer characteristics with the p-channel OFET as the load and the n-channel OFET as the driver. Reproduced with permission.[30] 2007, American Chemical Society. (c) Optical image (left, scale bar, 2 mm) and schematic illustration (right) of complementary inverter circuit array based on P3HT/PEO-blend NWs and P(NDI2OD-T2)/PEO-blend NWs (PMOS: p-channel metal-oxide-semiconductor FET, NMOS: n-channel metal-oxide-semiconductor FET). (d) Input–output voltage characteristic of ONW complementary inverter. Reproduced with permission.[109] 2013, Nature Publishing Group.

N2200)/PEO) by using an ENP technique (Figure 10): the exact numbers of wires, their orientations and their dimensions were controlled directly on the device substrate without any transfer printing process. They reported large-area printing of highly-aligned, individually-controlled NWs and showed high performance of the ONW transistors. The maximum mobility of P3HT NW FETs based on ion-gel gate dielectric layer with nanometer channel length is 9.7 $cm^2 \cdot V^{-1} \cdot s^{-1}$ (Figure 13c). Fabrication of highly-aligned, individually-controlled ONWs in large area is a promising approach to realize flexible or textile nano-electronics with high performance.

3.1.2. Complementary Logic Circuits

Organic electronic circuit applications have received considerable attention recently as the industrially expected values of organic electronics increase. Such complementary logic circuits using the ONWs outperform circuits consisted of only p- or n- type transistors with a key characteristic of low power consumption, implying significant advantages for large area circuit integration.

Briseno et al.[30] demonstrated complementary logic circuits using 1D organic semiconductors; the circuits were based on n-channel PTCDI NWs and p-channel HTP NWs synthesized by a solution-phase self-assembly. The authors combined PTCDI and HTP NW transistors for the complementary inverters by drop-casting NW/methanol solutions onto the electrodes. The highest electron and hole mobility values measured were 0.027 $cm^2 \cdot V^{-1} \cdot s^{-1}$ for PTCDI and 0.01 $cm^2 \cdot V^{-1} \cdot s^{-1}$ for HTP respectively, and complementary inverters based on the NWs achieved gains as high as 8 (**Figure 14**a,b). These results demonstrated the first example of the use of 1D organic semiconductors in complementary inverters.

In addition to organic NWs, inorganic NWs were used to fabricate hybrid circuits. Tang et al.[13] used CuPc, $F_{16}CuPc$ single-crystal NWs and conducting Sb-doped tin dioxide (SnO_2:Sb) NWs to construct hybrid circuits, and studied complementary circuits such as transfer gates, SRAMs, NOR gates, OR gates, NAND gates, and ambipolar transistors. The inverters showed sharp switching and high gain, and logic circuits demonstrated low operational voltage, low current and ultralow power consumption (< 40 pW).

Just recently, the large-area and flexible electronics based on ONWs were provided by Min et al.[109] as mentioned above. They demonstrated not only high performance ONW transistors but also complementary circuit array using well-aligned P3HT/PEO and P(NDI2OD-T2)/PEO NWs. The ONW complementary inverter showed the typical switching characteristic with gain of ~17 (Figure 14c,d). Development of various ONW electronic circuit applications find open new opportunities in organic nanoelectronics and highly sophisticated integrated logic devices.

3.2. Light-Emitting Devices and Lasers

A new concept of integrated circuits including optoelectronic modulators that transmit information using optical signals as well as electrical signals, is an innovative to process and

transport data. However, the current technological trend of decreasing size of electronic chips requires that the circuit components should be nanoscale size. Therefore, the nanoscale patterning of optical circuits containing light sources, waveguides and light amplifiers are essential. In this sense, ONWs can provide a promising structural model for nanoscale optical communication systems.

3.2.1. Light-Emitting Devices

In fact, an ONW is not a perfect form to be used as an active layer in light-emitting devices, mainly because ONWs are 1D structures. Electrical contact and efficient charge injection into ONWs can be easily hampered by their fiber-like morphologies.[6,128] Also, the vacancies between ONWs can lead to a short-circuit problem in the devices.[6] Furthermore, accurate control of layer thickness is more challenging in ONW-based light-emitting devices than in thin film-based devices. In spite of these challenges, many researchers are attempting to develop ONW-based light-emitting devices because they can be possibly used as nanoscale light emitters for optoelectronic integrated circuits and lab-on-a-chip devices[6,128] and can provide a chance to study anisotropic electroluminescence (EL) of organic materials.[129,130]

One approach for fabricating NW-based emission layer is to grow light-emitting NWs by PVT. Tris(8-hydroxyquinoline)aluminum single-crystalline NWs were prepared by adsorbent-assisted PVT and used as emission layers in light-emitting devices.[131] The NW device of 40-nm diameter showed the best external quantum efficiency (0.90% ph/el) which was close to that of a thin-film reference device (0.92% ph/el), although the NW device had significant leakage current at voltage <7 V.

Using organic/inorganic hybrid NWs grown by PVT as light-emitters provided an effective way to analyze the emission properties of organic materials with their aggregation and molecular packing.[129] PTCDI/ZnO hybrid NWs were prepared using PVT on indium tin oxide (ITO) substrates and incorporated in light-emitting devices. By filling the void between the NWs with insulating polymers the authors used PTCDI/ZnO hybrid NWs successfully used as emitters in light-emitting diodes without a short circuit problem. The NW-based light-emitting diodes showed a blue-white emission, not the broad red emission of PTCDI film or the UV emission of ZnO; this difference clearly demonstrated that energy transfer from ZnO to PTCDI occurred and can vary with their aggregation, and that the optical properties of organic materials can vary with their molecular packing. However, the specific device performance was totally not reported except for EL spectrum.

Also, the anisotropic emission properties of organic materials could be observed by rendering organic thin film uniaxially nanoconfined via nanoimprinting process. Polymer light-emitting diodes incorporating uniaxially nanoconfined poly(9,9-dioctylfluorene-co-benzothiadiazole) (F8BT) emission layers exhibited a highly-anisotropic EL with a polarization ratio of 11.[130]

ES is another useful process to fabricate ONW emission layers. ES enables to study emission properties of a single NW because it produces a continuous NW from the nozzle. Moran-Mirabal et al.[132] fabricated light-emitting NWs from ionic transition metal complexes (ruthenium (II) tris(bipyridine), iTMC) and PEO mixtures, and demonstrated EL with a highly-confined dimension of 240 × 325 nm from a single NW deposited on gold interdigitated electrodes (**Figure 15**a–c). Yang et al.[133] introduced coaxial ES to directly fabricate 1D electroluminescent devices (Figure 15d,e). Galinstan liquid metal inside iTMC/PEO mixtures served as cathode, and coated ITO outside served as an anode. The luminescence occurred along the coaxial NW device.

Electrospun non-woven NW mats can also be used as an emission layer in light-emitting devices. However, due to voids in the non-woven mats, treatments to prevent the short-circuit problem are highly required. Vohra et al.[134] reported EL from electrospun non-woven mats of F8BT/PEO blend NWs. They annealed the NWs deposited on ITO anode at 150 °C to flatten the emission layer and to extract PEO from the NWs. The extraction of PEO resulted in a high concentration of conjugated polymer with increased crystallinity, and allowed formation of an electrically-inactive layer which prevents the occurrence of short circuits. At 6 V, the reported external quantum efficiency was 1.1% ph/el and the luminance was 2300 cd·m^{-2}.

Although the above research results have demonstrated the potential of ONW-based light-emitting devices as nano-sized light-emitters, further developments should be achieved to increase the quantum efficiencies of the devices in terms of ONW fabrication processes and device structures. Furthermore, controlling the directions and orientations of the ONWs and narrowing the diameters of ONWs below 100 nm are required to rigorously study the 1D anisotropic EL properties of light-emitting ONWs.

3.2.2. Waveguides and Lasers

ONW can function as interconnects in optical circuits, as metal wires do in electronic circuits. Because the refractive indices of organic small molecules and polymers are generally in the range of 1.5–2, ONWs can transmit light by total internal reflection like optical fibers. Especially, the smooth surfaces and highly-stacked π-conjugated molecular structures of crystalline ONWs can help to minimize optical loss during light propagation by reducing the amount of escaped scattered light and by improving photon-crystal lattice interactions.[6,135,136] Many researchers have reported the waveguiding properties of ONWs fabricated using various methods including ES,[137–140] PVT[141] and template wetting.[142]

Also, 1D structure of ONWs can be exploited as uniaxial Fabry-Pérot cavity. Light amplification in ONWs gives an opportunity to overcome optical losses in photonic circuits.[128] To achieve lasing action in ONWs, they must consist of π-conjugated molecular compounds to allow excitation. Also, ONWs should have flat and smooth end facets for effective light reflection and oscillation.[6,128,136]

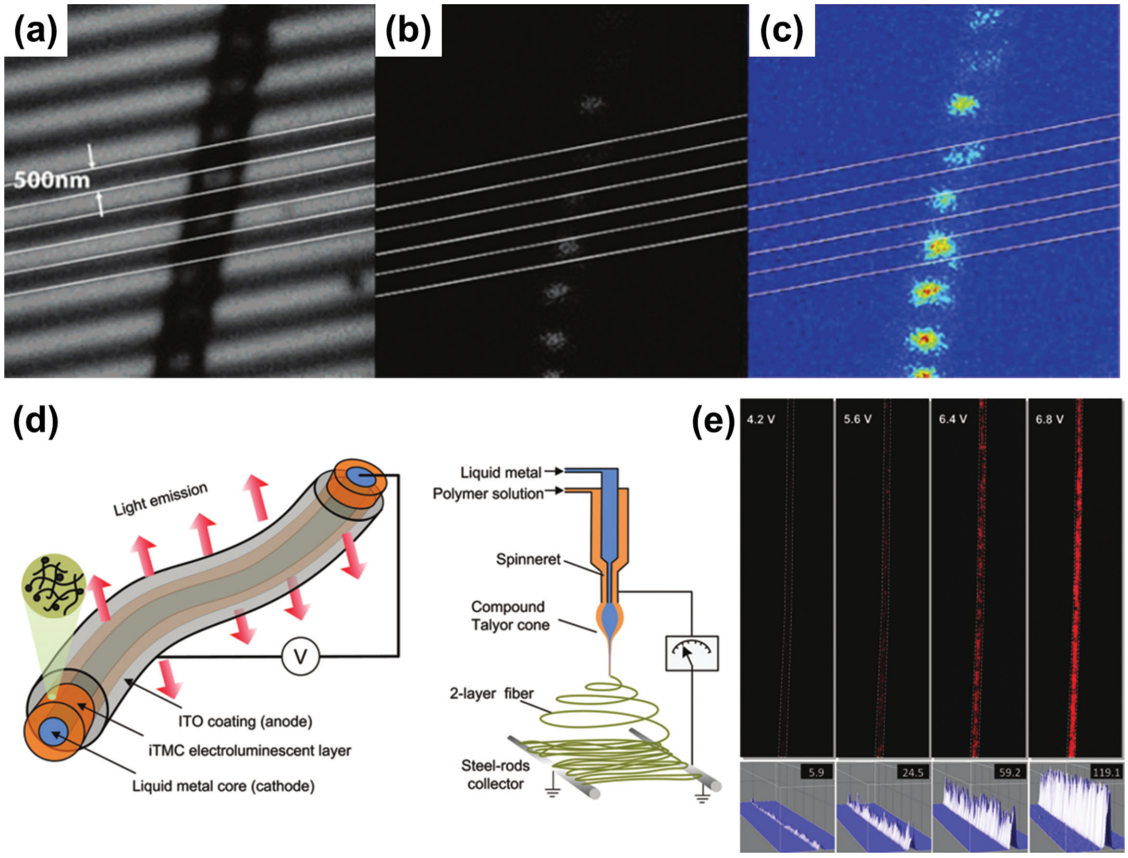

Figure 15. (a) Bright field image of an electrospun iTMC embedded PEO nanofiber crossing the interdigitated electrodes. Electrode gaps have been outlined. (b) Emission from fiber imaged in (a) at 4 V. (c) Pseudocolor rendition of (b) for comparison of intensity in individual gaps. Reproduced with permission.[132] 2007, American Chemical Society. (d) Schematic structure (left) of an iTMC-based electro-luminescent nanofiber and setup of coaxial ES (right). (e) Luminescence responses of the iTMC-based electro-luminescent nanofiber to different voltages applied to the device in N_2. Reproduced with permission.[133] 2012, American Chemical Society.

O'Carroll et al.[44] observed the optical microcavity behavior and optically pumped lasing in single π-conjugated polymer NWs (**Figure 16**). The authors used template-wetting to synthesize poly(9,9-dioctylfluorene) (PFO) NWs and measured spatially-resolved photoluminescence from the NW bodies and tips. The microcavity effects in PFO NWs were demonstrated by the observation that periodic intensity variations occurred in tip emission spectra, but not in body spectra (Figure 16a), and that dependence of mode spacing on the inverse of NW length was linear. Also, lasing action was observed with a single narrowed emission peak above the threshold pump energy of ~100 nJ (Figure 16b,c). The lasing action was also observed in single-crystal ONWs based on small organic molecules fabricated by adsorbent-assisted PVT.[143]

ES has many advantages for constructing ONW-based photonic systems because it enables control of ONW diameter and morphology, although control of individual NWs would be difficult unless a specially-designed experimental setup were introduced.[6,128] Camposeo et al. and Pagliara et al.[144,145] reported laser emission from electrospun poly(methyl methacrylate) NWs embedded with Rhodamine 6G, an organic fluorescent dye. ES can fabricate the ONWs with very high throughput, but addressability of position and orientation of electrospun NWs are inefficient. If ONWs can be directly prepared in desired positions and orientations using individual alignment methods, this ability will facilitate the formation of complex optoelectronic circuits. However, the realization of ONW-incorporating optoelectronic communication systems with waveguiding and laser emission in freely-patterned ONWs has not been reported yet.

3.3. Energy-Harvesting Devices

Recently, organic energy harvesting electronic devices for generating clean, sustainable and renewable energy have been investigated as replacements for carbon-based energy. Organic photovoltaics (OPVs) can convert solar energy to electrical energy and can be fabricated by a solution process, so lightweight, flexible, low-cost and large electronic devices can be produced.

The bulk heterojunction OPV is a promising device structure because it can provide a large interfacial area between donors and acceptors.[146] Based on enhanced exciton dissociation, this structure shows high short-circuit current density (J_{SC}). Organic 1D nanostructure materials have beneficial properties such as large surface-to-volume ratio, long exciton diffusion length, easy-to-control morphologies and high charge carrier mobility, so that power conversion efficiency

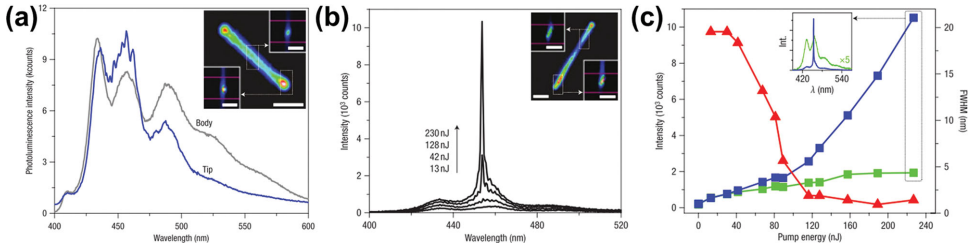

Figure 16. (a) Emission spectra collected from the tip (blue) and body (grey) of an isolated PFO NW under uniform pulsed excitation (1.4 nJ). Inset: emission image of an excited wire (1nJ). Scale bars, 2 μm. (b) Emission spectra collected from the tip of an isolated PFO NW under uniform excitation, as a function of increasing pump energy at room temperature. (c) Plot of the NW tip (blue squares) and body (green squares) emission peak intensity and full width at half maximum (FWHM, red triangles) versus pump energy for the wire shown in (b). Inset: above threshold (230 nJ) emission spectra acquired from the wire tip (blue) and body (green). Reproduced with permission.[44] 2007, Nature Publishing Group.

(PCE) can be improved. Also organic 1D materials are also solution-processible, so flexible devices can be fabricated.

1D structure nanomaterials in the bulk heterojunction OPVs have been formed in the various shapes such as nanofibers, nanopillars, nanoribbons, and 1D nanopattern.[11,25,26,45,60,61,63,147–154] Self-assembled 1D nanostructures are adjustable as donor material for organic solar cells because 1D donor material increases interfacial area with acceptor. Xin et al.[11a] produced active layer with p-type donor of self-assembled poly(3-butylthiophene) (P3BT) NW and n-type acceptor of fullerene solution, [6,6]-phenyl-C_{61}-butyric acid methyl ester (C_{61}-PCBM) and [6,6]-phenyl-C_{71}-butyric acid methyl ester (C_{71}-PCBM). They verified that P3BT NW/C_{61}-PCBM nanocomposite had higher field-effect hole mobility (8.0×10^{-3} $cm^2 \cdot V^{-1} \cdot s^{-1}$) than that of conventional P3BT/C_{61}-PCBM blends (3.8×10^{-5} $cm^2 \cdot V^{-1} \cdot s^{-1}$) using the FET characterization. Based on the better charge transport property, an OPV device consisting of P3BT NW/C_{61}-PCBM showed higher performance (J_{SC} = 7.68 $mA \cdot cm^{-2}$, fill factor (FF) = 57% and PCE = 2.2%) than did a device based on P3BT/C_{61}-PCBM blends (J_{SC} = 4.90 $mA \cdot cm^{-2}$, FF = 48% and PCE = 1.0%), and P3BT NW/C_{71}-PCBM and P3HT/C_{71}-PCBM blends showed similar PCE (3.0%) (**Figure 17**).

1D polymer nanostructures fabricated by AAO template method have partially more aligned polymer chain along the straight pore of the AAO during solidification of polymer solution, which can improve the performances of devices due to increased charge transport.[45] NIL also can produce 1D nanostructured donor for active layer of OPV devices. As increasing interfacial area between donor and acceptor by controlling the width of nanostructure, exciton capture is enhanced that produces high-efficiency solar cell devices.[149] By combining AAO template and nanoimprint methods, P3HT nanopillar arrays were fabricated on a deposited P3HT layer.[63] Compared to OPV devices based on P3HT bilayer film structure, larger contact area allowed more interaction between P3HT and PCBM, so J_{SC} of the device increased from 3.88 $mA \cdot cm^{-2}$ to 7.06 $mA \cdot cm^{-2}$ and PCE increased from 0.82% to 2.0% with 50-nm diameter nanopillars. A device that is consisted of smaller diameter (30 nm) nanopillars had higher performances with J_{SC} = 7.46 $mA \cdot cm^{-2}$, FF = 53.53% and PCE = 2.4% because exciton dissociation was more activated in the smaller nanopillar than in the large one.

ES is another effective method to fabricate the OPVs with semiconducting NWs. Based on properties of high aspect ratio and surface-to-volume ratio of electrospun NWs, large interfacial area can improve charge separation and transport. Sundarrajan et al.[147] and Bedford et al.[148] fabricated core/shell structured nanofibers using the coaxial ES method. The core was composed of active materials such as P3HT and C_{61}-PCBM, and the shell covered a core fiber with a high molecular polymer for sufficient chain entanglement which made well-connected nanofibers during ES. After removal of the polymer shell, a pure P3HT/C_{61}-PCBM nanofiber web was used as an active layer in the OPVs. OPVs based on electrospun P3HT/C_{61}-PCBM nanofibers showed quiet low performance ($J_{SC} = 3.2 \times 10^{-6}$ $mA \cdot cm^{-2}$, FF = 22.1% and PCE = 8.7×10^{-8} %) which was attributed to too thick (~5 μm) thickness of fiber networks to enable effective charge carrier transport.[147] To overcome the diffusion length issue of charge carriers, Bedford et al.[148] used a homogeneous solution of P3HT/C_{61}-PCBM to backfill pores in the nanofibers

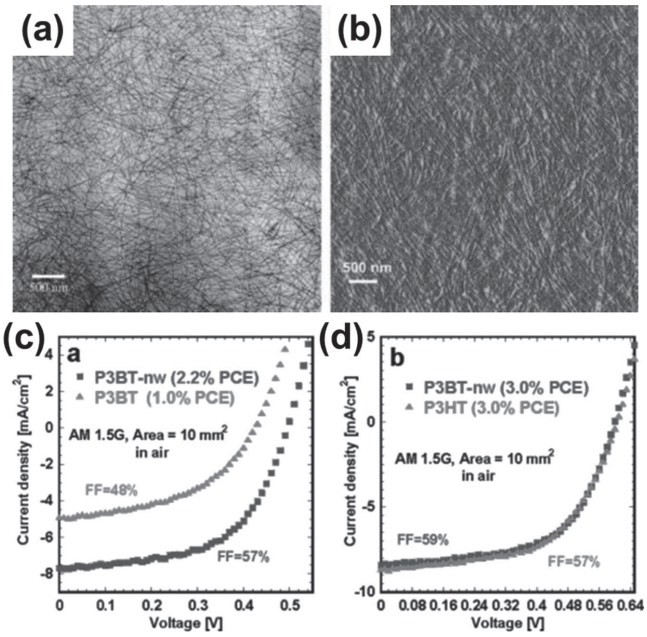

Figure 17. (a) TEM and (b) atomic force microscope images of P3BT NW/C_{61}-PCBM nanocomposites. The current–voltage characteristics of solar cells with different active layers: (c) P3BT NW/C_{61}-PCBM nanocomposite (70 nm) (blue squares) and P3BT/C_{61}-PCBM blend (80 nm) (red triangles); (d) P3BT NW/C_{71}-PCBM composite (90 nm) (blue squares), P3HT/C_{71}-PCBM blend (120 nm) (red triangles). Reproduced with permission.[11]2008, American Chemical Society.

and make the uniform active layer. Because the backfill layer significantly increased the interfacial area between donor and acceptor, the nanostructured OPV showed better performance than that of a P3HT/C_{61}-PCBM film device (J_{SC} = 10.7 mA·cm^{-2}, FF = 63% and PCE = 4%).

On the other hand, PVT process can be used to develop high-performance OPV devices based on p-n junction of organic single-crystalline 1D nanostructures. Zhang et al.[25] demonstrated the p-n junction nanoribbons with CuPc and F_{16}CuPc and achieved the p-n junction photovoltaic device. Due to their similar lattice constant, molecular structures and π–π stacking direction between two materials, F_{16}CuPc can be successfully grown onto CuPc nanoribbons. They proved the characteristics of p-n junction nanoribbons by fabricating an ambipolar FET; the device showed V-shaped transfer characteristics and balanced field-effect mobilities of 0.07 cm^2·V^{-1}·s^{-1} in the CuPc (p-type) and 0.05 cm^2·V^{-1}·s^{-1} in the F_{16}CuPc (n-type). This balance between hole and electron mobilities assisted charge carrier transport properties in the solar cell. The photovoltaic device had J_{SC} = 0.054 mA·cm^{-2}, FF = 36% and PCE = 0.007%, which are relatively low, but it was a meaningful study for understanding the fundamentals of OPVs.

Many research for photovoltaic devices using organic 1D nanostructures have been reported with their advantages of large interfacial area between donors and acceptors which improve the charge separation and enhance charge transport properties. However, conventional OPVs based on ONWs instead of organic thin film as the active layer are limited in the improvement of performances. Therefore, an innovative structure only for NW-based devices is essential to achieve the highly-efficient photovoltaics with distinctive properties of ONWs.

4. Conclusion

In this review, we summarized ONW fabrication methods from the perspective of possibility and strategy of alignment, and the various electronic and photonic applications such as FETs, circuits, light-emitting devices, waveguides, and photovoltaic devices. ONWs are interesting materials because they can be used both as building blocks of nanoscale devices with high performance and high-efficiency, and as a model of theoretical studies to investigate charge transport mechanisms.

Various fabrication techniques and device applications of ONWs have been reported, but some problems remain to be solved. A technique that perfectly satisfies the requirements (alignment; individually-controlled patterning; reproducibility; and controllability of wire morphology and chain orientation) for practical device applications should be developed. For instance, the recently-reported ENP technique is most suitable for industrial applications of ONWs because it can individually control and align the wires, and using this method enables controlling and analyzing the wire morphology and chain orientation. Furthermore, the performance of ONW-based electronics devices has been increased consistently, but the main objective of the studies has been to match the properties of counterpart devices based on inorganic materials. Applications of only ONWs that use the most of their unique characteristics are hardly ever reported.

Efforts to develop a device with innovative concept and structure that exploits the distinctive characteristics of 1D organic nanostructure is required, as opposed to just substituting 1D structures for 2D or 3D bulk materials in conventional device structures. Such investigations could improve the competitiveness of organic materials and devices for the next-generation electronics, and could advance the realization of future flexible and stretchable electronics.

Acknowledgements

This work was supported by a grant (Code No. 2013M3A6A5073175) from the Center for Advanced Soft Electronics under the Global Frontier Research Program of the Ministry of Science, ICT & Future Planning, Korea. This research was also supported by the Basic Research Program through the National Research Foundation (NRF) of Korea, funded by the Ministry of Education (NRF-2013R1A1A2012660), Korea. This study was also supported by Brain Korea 21 PLUS project for Center for Creative Industrial Materials.

[1] Y. Xia, P. Yang, Y. Sun, Y. Wu, B. Mayers, B. Gates, Y. Yin, F. Kim, H. Yan, *Adv. Mater.* **2003**, *15*, 353.
[2] K. Takei, T. Takahashi, J. C. Ho, H. Ko, A. G. Gillies, P. W. Leu, R. S. Fearing, A. Javey, *Nat. Mater.* **2010**, *9*, 821.
[3] T. Sekitani, Y. Noguchi, K. Hata, T. Fukushima, T. Aida, T. Someya, *Science* **2008**, *321*, 1468.
[4] A. L. Briseno, S. C. B. Mannsfeld, S. A. Jenekhe, Z. Bao, Y. Xia, *Mater. Today* **2008**, *11*, 38.
[5] L. Zang, Y. Che, J. S. Moore, *Acc. Chem. Res.* **2008**, *41*, 1596.
[6] H. Cho, S.-Y. Min, T.-W. Lee, *Macromol. Mater. Eng.* **2013**, *298*, 475.
[7] D. H. Kim, D. Y. Lee, H. S. Lee, W. H. Lee, Y. H. Kim, J. I. Han, K. Cho, *Adv. Mater.* **2007**, *19*, 678.
[8] J. H. Oh, H. W. Lee, S. Mannsfeld, R. M. Stoltenberg, E. Jung, Y. W. Jin, J. M. Kim, J.-B. Yoo, Z. Bao, *Proc. Natl. Acad. Sci. USA* **2009**, *106*, 6065.
[9] A. N. Aleshin, *Adv. Mater.* **2006**, *18*, 17.
[10] J. A. Merlo, C. D. Frisbie, *J. Phys. Chem. B* **2004**, *108*, 19169.
[11] a) H. Xin, F. S. Kim, S. A. Jenekhe, *J. Am. Chem. Soc.* **2008**, *130*, 5424; b) P.-H. Wang, H.-F. Lee, Y.-C. Huang, Y.-J. Jung, F.-L. Gong, W.-Y. Huang, *Electron. Mater. Lett.* **2014**, *10*, 767.
[12] J. Chang, M. Dommer, C. Chang, L. Lin, *Nano Energy* **2012**, *1*, 356.
[13] Q. Tang, Y. Tong, W. Hu, Q. Wan, T. Bjørnholm, *Adv. Mater.* **2009**, *21*, 4234.
[14] M. Steinhart, R. B. Wehrspohn, U. Gösele, J. H. Wendorff, *Angew. Chem. Int. Ed.* **2004**, *43*, 1334.
[15] M. Steinhart, J. H. Wendorff, A. Greiner, R. B. Wehrspohn, K. Nielsch, J. Schilling, J. Choi, U. Gösele, *Science* **2002**, *296*, 1997.
[16] Y. Xia, G. M. Whitesides, *Angew. Chem. Int. Ed.* **1998**, *37*, 550.
[17] a) J. Shui, J. C. M. Li, *Nano Lett.* **2009**, *9*, 1307; b) P. Frontera, S. Trocino, A. Donato, P. L. Antonucci, M. L. Faro, G. Squadrito,

G. Neri, *Electron. Mater. Lett.* **2014**, *10*, 305; c) H.-W. Cui, X. Tang, *Electron. Mater. Lett.* **2014**, *10*, 183.
[18] C. Kloc, P. G. Simpkins, T. Siegrist, R. A. Laudise, *J. Cryst. Growth* **1997**, *182*, 416.
[19] V. C. Sundar, J. Zaumseil, V. Podzorov, E. Menard, R. L. Willett, T. Someya, M. E. Gershenson, J. A. Rogers, *Science* **2004**, *303*, 1644.
[20] A. L. Briseno, S. C. B. Mannsfeld, M. M. Ling, S. Liu, R. J. Tseng, C. Reese, M. E. Roberts, Y. Yang, F. Wudl, Z. Bao, *Nature* **2006**, *444*, 913.
[21] J. E. Park, M. Son, M. Hong, G. Lee, H. C. Choi, *Angew. Chem. Int. Ed.* **2012**, *51*, 6383.
[22] Q. Tang, H. Li, M. He, W. Hu, C. Liu, K. Chen, C. Wang, Y. Liu, D. Zhu, *Adv. Mater.* **2006**, *18*, 65.
[23] Q. Tang, H. Li, Y. Liu, W. Hu, *J. Am. Chem. Soc.* **2006**, *128*, 14634.
[24] Q. Tang, Y. Tong, H. Li, Z. Ji, L. Li, W. Hu, Y. Liu, D. Zhu, *Adv. Mater.* **2008**, *20*, 1511.
[25] Y. Zhang, H. Dong, Q. Tang, S. Ferdous, F. Liu, S. C. B. Mannsfeld, W. Hu, A. L. Briseno, *J. Am. Chem. Soc.* **2010**, *132*, 11580.
[26] Q. H. Cui, L. Jiang, C. Zhang, Y. S. Zhao, W. Hu, J. Yao, *Adv. Mater.* **2012**, *24*, 2332.
[27] V. Podzorov, E. Menard, A. Borissov, V. Kiryukhin, J. A. Rogers, M. E. Gershenson, *Phys. Rev. Lett.* **2004**, *93*, 086602.
[28] A. L. Briseno, S. C. B. Mannsfeld, X. Lu, Y. Xiong, S. A. Jenekhe, Z. Bao, Y. Xia, *Nano Lett.* **2007**, *7*, 668.
[29] K. Balakrishnan, A. Datar, R. Oitker, H. Chen, J. Zuo, L. Zang, *J. Am. Chem. Soc.* **2005**, *127*, 10496.
[30] A. L. Briseno, S. C. B. Mannsfeld, C. Reese, J. M. Hancock, Y. Xiong, S. A. Jenekhe, Z. Bao, Y. Xia, *Nano Lett.* **2007**, *7*, 2847.
[31] L. Qiu, W. H. Lee, X. Wang, J. S. Kim, J. A. Lim, D. Kwak, S. Lee, K. Cho, *Adv. Mater.* **2009**, *21*, 1349.
[32] J. A. Lim, J.-H. Kim, L. Qiu, W. H. Lee, H. S. Lee, D. Kwak, K. Cho, *Adv. Funct. Mater.* **2010**, *20*, 3292.
[33] Y. Che, X. Yang, S. Loser, L. Zang, *Nano Lett.* **2008**, *8*, 2219.
[34] K. Balakrishnan, A. Datar, W. Zhang, X. Yang, T. Naddo, J. Huang, J. Zuo, M. Yen, J. S. Moore, L. Zang, *J. Am. Chem. Soc.* **2006**, *128*, 6576.
[35] J. C. Hulteen, C. R. Martin, *J. Mater. Chem.* **1997**, *7*, 1075.
[36] C. Schönenberger, B. M. I. van der Zande, L. G. J. Fokkink, M. Henny, C. Schmid, M. Krüger, A. Bachtold, R. Huber, H. Birk, U. Staufer, *J. Phys. Chem. B* **1997**, *101*, 5497.
[37] B. B. Lakshmi, C. J. Patrissi, C. R. Martin, *Chem. Mater.* **1997**, *9*, 2544.
[38] S. J. Limmer, S. Seraji, M. J. Forbess, Y. Wu, T. P. Chou, C. Nguyen, G. Z. Cao, *Adv. Mater.* **2001**, *13*, 1269.
[39] S. J. Limmer, G. Cao, *Adv. Mater.* **2003**, *15*, 427.
[40] Y.-K. Su, D.-H. Qin, H.-L. Zhang, H. Li, H.-L. Li, *Chem. Phys. Lett.* **2004**, *388*, 406.
[41] S. J. Limmer, S. Seraji, Y. Wu, T. P. Chou, C. Nguyen, G. Z. Cao, *Adv. Funct. Mater.* **2002**, *12*, 59.
[42] Y. C. Wang, I. C. Leu, M. H. Hon, *J. Mater. Chem.* **2002**, *12*, 2439.
[43] H.-B. Xu, H.-Z. Chen, W.-J. Xu, M. Wang, *Chem. Phys. Lett.* **2005**, *412*, 294.
[44] D. O'Carroll, I. Lieberwirth, G. Redmond, *Nat. Nanotechnol.* **2007**, *2*, 180.
[45] H.-S. Wang, L.-H. Lin, S.-Y. Chen, Y.-L. Wang, K.-H. Wei, *Nanotechnology* **2009**, *20*, 075201.
[46] J.-T. Chen, M. Zhang, T. P. Russell, *Nano Lett.* **2007**, *7*, 183.
[47] S. H. Lee, D. H. Park, K. Kim, J. Joo, D.-C. Kim, H.-J. Kim, J. Kim, *Appl. Phys. Lett.* **2007**, *91*, 263102.
[48] L. Piraux, S. Dubois, S. Demoustier-Champagne, *Nucl. Instruments Methods Phys. Res. Sect. B Beam Interact. with Mater. Atoms* **1997**, *131*, 357.
[49] M. Zhang, P. Dobriyal, J.-T. Chen, T. P. Russell, J. Olmo, A. Merry, *Nano Lett.* **2006**, *6*, 1075.
[50] C. Wang, Z. Wang, M. Li, H. Li, *Chem. Phys. Lett.* **2001**, *341*, 431.
[51] Z. Fan, J. C. Ho, Z. A. Jacobson, R. Yerushalmi, R. L. Alley, H. Razavi, A. Javey, *Nano Lett.* **2008**, *8*, 20.
[52] X.-M. Zhao, Y. Xia, G. M. Whitesides, *J. Mater. Chem.* **1997**, *7*, 1069.
[53] Y. Xia, J. Tien, D. Qin, G. M. Whitesides, *Langmuir* **1996**, *12*, 4033.
[54] Y. Xia, J. J. McClelland, R. Gupta, D. Qin, X.-M. Zhao, L. L. Sohn, R. J. Celotta, G. M. Whitesides, *Adv. Mater.* **1997**, *9*, 147.
[55] S. Y. Chou, P. R. Krauss, P. J. Renstrom, *Appl. Phys. Lett.* **1995**, *67*, 3114.
[56] W. Zhang, S. Y. Chou, *Appl. Phys. Lett.* **2003**, *83*, 1632.
[57] S. Y. Chou, P. R. Krauss, P. J. Renstrom, *Science* **1996**, *272*, 85.
[58] M. D. Austin, H. Ge, W. Wu, M. Li, Z. Yu, D. Wasserman, S. A. Lyon, S. Y. Chou, *Appl. Phys. Lett.* **2004**, *84*, 5299.
[59] M. Aryal, K. Trivedi, W. (Walter) Hu, *ACS Nano* **2009**, *3*, 3085.
[60] M. Aryal, F. Buyukserin, K. Mielczarek, X.-M. Zhao, J. Gao, A. Zakhidov, W. (Walter) Hu, *J. Vac. Sci. Technol. B* **2008**, *26*, 2562.
[61] D. Cheyns, K. Vasseur, C. Rolin, J. Genoe, J. Poortmans, P. Heremans, *Nanotechnology* **2008**, *19*, 424016.
[62] D. Cui, H. Li, H. Park, X. Cheng, *J. Vac. Sci. Technol. B* **2008**, *26*, 2404.
[63] D. Chen, W. Zhao, T. P. Russell, *ACS Nano* **2012**, *6*, 1479.
[64] B. D. Gates, Q. Xu, M. Stewart, D. Ryan, C. G. Willson, G. M. Whitesides, *Chem. Rev.* **2005**, *105*, 1171.
[65] X.-M. Zhao, Y. Xia, G. M. Whitesides, *Adv. Mater.* **1996**, *8*, 837.
[66] H. Yang, P. Deschatelets, S. T. Brittain, G. M. Whitesides, *Adv. Mater.* **2001**, *13*, 54.
[67] L. J. Guo, *Adv. Mater.* **2007**, *19*, 495.
[68] X. Duan, Y. Zhao, E. Berenschot, N. R. Tas, D. N. Reinhoudt, J. Huskens, *Adv. Funct. Mater.* **2010**, *20*, 2519.
[69] E. Kim, Y. Xia, G. M. Whitesides, *Nature* **1995**, *376*, 581.
[70] J. K. Hwang, S. Cho, J. M. Dang, E. B. Kwak, K. Song, J. Moon, M. M. Sung, *Nat. Nanotechnol.* **2010**, *5*, 742.
[71] D. Li, Y. Xia, *Adv. Mater.* **2004**, *16*, 1151.
[72] D. H. Reneker, A. L. Yarin, H. Fong, S. Koombhongse, *J. Appl. Phys.* **2000**, *87*, 4531.
[73] A. L. Yarin, S. Koombhongse, D. H. Reneker, *J. Appl. Phys.* **2001**, *90*, 4836.
[74] V. Thavasi, G. Singh, S. Ramakrishna, *Energy Environ. Sci.* **2008**, *1*, 205.
[75] S. Kaur, R. Gopal, W. J. Ng, S. Ramakrishna, T. Matsuura, *MRS Bull.* **2008**, *33*, 21.
[76] R. S. Barhate, S. Ramakrishna, *J. Memb. Sci.* **2007**, *296*, 1.
[77] R. Gopal, S. Kaur, Z. Ma, C. Chan, S. Ramakrishna, T. Matsuura, *J. Memb. Sci.* **2006**, *281*, 581.
[78] S. Kaur, Z. Ma, R. Gopal, G. Singh, S. Ramakrishna, T. Matsuura, *Langmuir* **2007**, *23*, 13085.
[79] S. Arumuganathar, S. N. Jayasinghe, *Biomed. Mater.* **2007**, *2*, 189.
[80] H.-J. Jin, J. Chen, V. Karageorgiou, G. H. Altman, D. L. Kaplan, *Biomaterials* **2004**, *25*, 1039.
[81] K. Yoshimatsu, L. Ye, J. Lindberg, I. S. Chronakis, *Biosens. Bioelectron.* **2008**, *23*, 1208.
[82] I. S. Chronakis, A. Jakob, B. Hagström, L. Ye, *Langmuir* **2006**, *22*, 8960.
[83] I.-D. Kim, A. Rothschild, B. H. Lee, D. Y. Kim, S. M. Jo, H. L. Tuller, *Nano Lett.* **2006**, *6*, 2009.
[84] S. F. Fennessey, R. J. Farris, *Polymer* **2004**, *45*, 4217.
[85] H. Pan, L. Li, L. Hu, X. Cui, *Polymer* **2006**, *47*, 4901.
[86] J. A. Matthews, G. E. Wnek, D. G. Simpson, G. L. Bowlin, *Biomacromolecules* **2002**, *3*, 232.
[87] B. Sundaray, V. Subramanian, T. S. Natarajan, R.-Z. Xiang, C.-C. Chang, W.-S. Fann, *Appl. Phys. Lett.* **2004**, *84*, 1222.
[88] D. Li, Y. Wang, Y. Xia, *Nano Lett.* **2003**, *3*, 1167.
[89] D. Li, Y. Wang, Y. Xia, *Adv. Mater.* **2004**, *16*, 361.
[90] W. E. Teo, S. Ramakrishna, *Nanotechnology* **2005**, *16*, 1878.

[91] M. V. Kakade, S. Givens, K. Gardner, K. H. Lee, D. B. Chase, J. F. Rabolt, *J. Am. Chem. Soc.* **2007**, *129*, 2777.
[92] R. Jalili, M. Morshed, S. A. H. Ravandi, *J. Appl. Polym. Sci.* **2006**, *101*, 4350.
[93] S. Lee, G. D. Moon, U. Jeong, *J. Mater. Chem.* **2009**, *19*, 743.
[94] S. W. Lee, H. J. Lee, J. H. Choi, W. G. Koh, J. M. Myoung, J. H. Hur, J. J. Park, J. H. Cho, U. Jeong, *Nano Lett.* **2010**, *10*, 347.
[95] J. Deitzel, J. Kleinmeyer, J. Hirvonen, N. B. Tan, *Polymer* **2001**, *42*, 8163.
[96] X. Cui, L. Li, F. Xu, *Appl. Phys. A* **2010**, *103*, 167.
[97] Y. Ishii, H. Sakai, H. Murata, *Mater. Lett.* **2008**, *62*, 3370.
[98] D. Yang, B. Lu, Y. Zhao, X. Jiang, *Adv. Mater.* **2007**, *19*, 3702.
[99] R. D. Piner, J. Zhu, F. Xu, S. Hong, C. A. Mirkin, *Science* **1999**, *283*, 661.
[100] D. S. Ginger, H. Zhang, C. A. Mirkin, *Angew. Chem. Int. Ed.* **2004**, *43*, 30.
[101] A. P. Suryavanshi, M.-F. Yu, *Nanotechnology* **2007**, *18*, 105305.
[102] G. M. Gratson, M. Xu, J. A. Lewis, *Nature* **2004**, *428*, 386.
[103] B. Y. Ahn, E. B. Duoss, M. J. Motala, X. Guo, S.-I. Park, Y. Xiong, J. Yoon, R. G. Nuzzo, J. A. Rogers, J. A. Lewis, *Science* **2009**, *323*, 1590.
[104] S. T. Parker, P. Domachuk, J. Amsden, J. Bressner, J. A. Lewis, D. L. Kaplan, F. G. Omenetto, *Adv. Mater.* **2009**, *21*, 2411.
[105] A. P. Suryavanshi, M.-F. Yu, *Appl. Phys. Lett.* **2006**, *88*, 083103.
[106] J. Hu, M.-F. Yu, *Science* **2010**, *329*, 313.
[107] J. T. Kim, S. K. Seol, J. Pyo, J. S. Lee, J. H. Je, G. Margaritondo, *Adv. Mater.* **2011**, *23*, 1968.
[108] J. T. Kim, J. Pyo, J. Rho, J.-H. Ahn, J. H. Je, G. Margaritondo, *ACS Macro Lett.* **2012**, *1*, 375.
[109] S.-Y. Min, T.-S. Kim, B. J. Kim, H. Cho, Y.-Y. Noh, H. Yang, J. H. Cho, T.-W. Lee, *Nat. Commun.* **2013**, *4*, 1773.
[110] D. Sun, C. Chang, S. Li, L. Lin, *Nano Lett.* **2006**, *6*, 839.
[111] C. Chang, K. Limkrailassiri, L. Lin, *Appl. Phys. Lett.* **2008**, *93*, 123111.
[112] Y. Sun, L. Tan, S. Jiang, H. Qian, Z. Wang, D. Yan, C. Di, Y. Wang, W. Wu, G. Yu, S. Yan, C. Wang, W. Hu, Y. Liu, D. Zhu, *J. Am. Chem. Soc.* **2007**, *129*, 1882.
[113] L. Jiang, J. Gao, E. Wang, H. Li, Z. Wang, W. Hu, L. Jiang, *Adv. Mater.* **2008**, *20*, 2735.
[114] R. Zeis, T. Siegrist, C. Kloc, *Appl. Phys. Lett.* **2005**, *86*, 022103.
[115] X. Zhang, G. Yuan, Q. Li, B. Wang, X. Zhang, R. Zhang, J. C. Chang, C. Lee, S. Lee, *Chem. Mater.* **2008**, *20*, 6945.
[116] S. Zhang, Y. Guo, Y. Zhang, R. Liu, Q. Li, X. Zhan, Y. Liu, W. Hu, *Chem. Commun.* **2010**, *46*, 2841.
[117] W. Jiang, Y. Zhou, H. Geng, S. Jiang, S. Yan, W. Hu, Z. Wang, Z. Shuai, J. Pei, *J. Am. Chem. Soc.* **2011**, *133*, 1.
[118] A. L. Briseno, Q. Miao, M.-M. Ling, C. Reese, H. Meng, Z. Bao, F. Wudl, *J. Am. Chem. Soc.* **2006**, *128*, 15576.
[119] K. S. Park, B. Cho, J. Baek, J. K. Hwang, H. Lee, M. M. Sung, *Adv. Funct. Mater.* **2013**, *23*, 4776.
[120] K. S. Park, S. M. Salunkhe, I. Lim, C.-G. Cho, S.-H. Han, M. M. Sung, *Adv. Mater.* **2013**, *25*, 3351.
[121] A. L. Briseno, S. C. B. Mannsfeld, P. J. Shamberger, F. S. Ohuchi, Z. Bao, S. A. Jenekhe, Y. Xia, *Chem. Mater.* **2008**, *20*, 4712.
[122] W. D. Oosterbaan, J.-C. Bolsée, A. Gadisa, V. Vrindts, S. Bertho, J. D'Haen, T. J. Cleij, L. Lutsen, C. R. McNeill, L. Thomsen, J. V Manca, D. Vanderzande, *Adv. Funct. Mater.* **2010**, *20*, 792.
[123] N. J. Pinto, A. T. Johnson, A. G. MacDiarmid, C. H. Mueller, N. Theofylaktos, D. C. Robinson, F. A. Miranda, *Appl. Phys. Lett.* **2003**, *83*, 4244.
[124] R. González, N. J. Pinto, *Synth. Met.* **2005**, *151*, 275.
[125] H. Liu, C. H. Reccius, H. G. Craighead, *Appl. Phys. Lett.* **2005**, *87*, 253106.
[126] J.-Y. Chen, C.-C. Kuo, C.-S. Lai, W.-C. Chen, H.-L. Chen, *Macromolecules* **2011**, *44*, 2883.
[127] C. J. Lin, J. C. Hsu, J. H. Tsai, C. C. Kuo, W. Y. Lee, W. C. Chen, *Macromol. Chem. Phys.* **2011**, *212*, 2452.
[128] A. Camposeo, L. Persano, D. Pisignano, *Macromol. Mater. Eng.* **2013**, *298*, 487.
[129] A. M. -C. Ng, A. B. Djurišić, K.-H. Tam, W.-M. Kwok, W.-K. Chan, W. Y. Tam, D. L. Phillips, K.-W. Cheah, *Adv. Funct. Mater.* **2008**, *18*, 566.
[130] Z. Zheng, K.-H. Yim, M. S. M. Saifullah, M. E. Welland, R. H. Friend, J.-S. Kim, W. T. S. Huck, *Nano Lett.* **2007**, *7*, 987.
[131] Y. S. Zhao, C. Di, W. Yang, G. Yu, Y. Liu, J. Yao, *Adv. Funct. Mater.* **2006**, *16*, 1985.
[132] J. M. Moran-Mirabal, J. D. Slinker, J. A. DeFranco, S. S. Verbridge, R. Ilic, S. Flores-Torres, H. Abruña, G. G. Malliaras, H. G. Craighead, *Nano Lett.* **2007**, *7*, 458.
[133] H. Yang, C. R. Lightner, L. Dong, *ACS Nano* **2012**, *6*, 622.
[134] V. Vohra, U. Giovanella, R. Tubino, H. Murata, C. Botta, *ACS Nano* **2011**, *5*, 5572.
[135] Q. H. Cui, Y. S. Zhao, J. Yao, *J. Mater. Chem.* **2012**, *22*, 4136.
[136] F. S. Kim, G. Ren, S. A. Jenekhe, *Chem. Mater.* **2011**, *23*, 682.
[137] H. Liu, J. B. Edel, L. M. Bellan, H. G. Craighead, *Small* **2006**, *2*, 495.
[138] F. Di Benedetto, A. Camposeo, S. Pagliara, E. Mele, L. Persano, R. Stabile, R. Cingolani, D. Pisignano, *Nat. Nanotechnol.* **2008**, *3*, 614.
[139] K. P. Dhakal, H. Lee, J. Woo Lee, J. Joo, M. Guthold, J. Kim, *J. Appl. Phys.* **2012**, *111*, 123504.
[140] L. Li, X. Yang, L. Yuan, *Mater. Lett.* **2012**, *66*, 292.
[141] Y. S. Zhao, P. Zhan, J. Kim, C. Sun, J. Huang, *ACS Nano* **2010**, *4*, 1630.
[142] D. O'Carroll, I. Lieberwirth, G. Redmond, *Small* **2007**, *3*, 1178.
[143] Y. S. Zhao, A. Peng, H. Fu, Y. Ma, J. Yao, *Adv. Mater.* **2008**, *20*, 1661.
[144] A. Camposeo, F. Di Benedetto, R. Stabile, A. A. R. Neves, R. Cingolani, D. Pisignano, *Small* **2009**, *5*, 562.
[145] S. Pagliara, A. Camposeo, F. Di Benedetto, A. Polini, E. Mele, L. Persano, R. Cingolani, D. Pisignano, *Superlattices Microst.* **2010**, *47*, 145.
[146] a) D.-H. Kim, K.-G. Lim, J. H. Park, T.-W. Lee, *Chem Sus Chem* **2012**, *5*, 2053; b) K.-G. Lim, M.-R. Choi, H.-B. Kim, J. H. Park, T.-W. Lee, *J. Mater. Chem.* **2012**, *22*, 25148; c) K.-G. Lim, M.-R. Choi, J.-H. Kim, D. H. Kim, G. H. Jung, Y. Park, J.-L. Lee, T.-W. Lee, *Chem Sus Chem* **2014**, *7*, 1125; d) M.-R. Choi, T.-H. Han, K.-G. Lim, S.-H. Woo, D. H. Huh, T.-W. Lee, *Angew. Chem. Int. Ed.* **2011**, *50*, 6274.
[147] S. Sundarrajan, R. Murugan, A. S. Nair, S. Ramakrishna, *Mater. Lett.* **2010**, *64*, 2369.
[148] N. M. Bedford, M. B. Dickerson, L. F. Drummy, H. Koerner, K. M. Singh, M. C. Vasudev, M. F. Durstock, R. R. Naik, A. J. Steckl, *Adv. Energy Mater.* **2012**, *2*, 1136.
[149] M.-S. Kim, J.-S. Kim, J. C. Cho, M. Shtein, J. Kim, L. J. Guo, *Appl. Phys. Lett.* **2007**, *90*, 123113.
[150] S. Karak, S. K. Ray, A. Dhar, *Appl. Phys. Lett.* **2010**, *97*, 043306.
[151] S. Berson, R. De Bettignies, S. Bailly, S. Guillerez, *Adv. Funct. Mater.* **2007**, *17*, 1377.
[152] S. Bertho, W. D. Oosterbaan, V. Vrindts, J. D'Haen, T. J. Cleij, L. Lutsen, J. Manca, D. Vanderzande, *Org. Electron.* **2009**, *10*, 1248.
[153] H. Xin, O. G. Reid, G. Ren, F. S. Kim, D. S. Ginger, S. A. Jenekhe, *ACS Nano* **2010**, *4*, 1861.
[154] T. Salim, S. Sun, L. H. Wong, L. Xi, Y. L. Foo, Y. M. Lam, *J. Phys. Chem. C* **2010**, *114*, 9459.

Received: May 27, 2014
Revised: August 6, 2014
Published online: October 6, 2014